

**Recording and measuring the shape of old-growth giant  
trees using UAV images**

**UAV 画像を用いた巨木の記録と形状計測**

Graduate School of Bioresources, Mie University  
Department of Environment Science and Technology  
Forest Operation and Systems  
Kaili Huang

## **Abstract**

The old-growth and giant tree is a nonrenewable resource with great value. However, old-growth giant trees are now at risk of falling due to aging and external pressures such as typhoons. In Japan, since some of the old-growth giant trees are located close to residential areas, damage from fallen trees can be severe in these areas. Moreover, as a symbol of the local community, the giant trees have great meaning to the local people. Therefore, it is important to check and record their periodic growth conditions. The purpose of this study was to record and measure the entire tree using aerial images taken by UAV from multiple directions. As a trial, Japanese larch (*Larix kaempfer*) and Japanese cedar (*Cryptomeria japonica*) located in Mie University Forest were recorded and analyzed. Orthophotos, dense clouds and 3D models of the tree were generated by SfM technology. The measurement from the reconstructions of the tree showed that tree height and DBH could be measured with relatively high accuracy using UAV images taken from the sides. This method was later promoted at Mt.Nonobori. An old-growth and giant Japanese cedar was recorded and measured. The measurements in different directions in our remote method differed from ground measurements by a range of 0 cm to 12 cm in DBHs and tree heights by a range of 3 m to 7 m. The results of this study showed that UAVs could be useful in recording the tree shape and measuring the tree structure parameters of the old-growth giant tree.

**Keywords:** DBH, Japanese larch, Japanese cedar, Structure from Motion, Tree height

## Table of content

1. Introduction	4
2. Materials and Methods	6
2.1 Sites and focal trees	6
2.1.1 Japanese larch and Japanese cedar in Mie University Forest	6
2.1.2 Old-growth and giant Japanese cedar in Mt. Nonobori	7
2.2 Photo capture	7
2.2.1 TELLO	7
2.2.2 BLUEGRASS FIELDS	8
2.2.3 Flight in Mie University Forest	8
2.2.4 Flight in Mt. Nonobori	9
2.3 Photo processing	10
2.4 Validating accuracy	11
2.4.1 Tree heights and DBHs obtained from orthophotos, dense clouds and 3D models	11
2.4.2 Ground Data Acquisition	12
2.4.3 Data Analysis	12
3. Results	13
3.1 Japanese larch and cedar in Mie University Forest	13
3.1.1 Orthophotos, Dense Cloud, 3D Model of the Japanese larch	13
3.1.2 Tree heights and DBHs of the Japanese larch	13
3.1.3 Orthophotos, Dense Cloud, 3D Model of the Japanese cedar	14
3.1.4 Tree heights and DBHs of the Japanese cedar	15
3.2 Old-growth giant Japanese cedar in Mt. Nonobori	16
3.2.1 Orthophotos, Dense Cloud, 3D Model	16
3.2.2 Tree heights and DBHs	17
4. Discussion	19

4.1 Characteristics of tree heights and DBHs by measurement methods .....	19
4.2 Environments of data acquisition .....	21
4.3 Benefit from citizen volunteers .....	22
5. Conclusion .....	24
Acknowledgment .....	25
References .....	26
List of tables .....	32
List of figures .....	33

## 1. Introduction

The old-growth giant tree is a nonrenewable resource for all countries with great value such as economic, cultural history, growing place, tree state, tree form, tree vigor, protection level, growth environment, tree species, tree canopy, and so on (Becker and Freeman, 2009; Blicharska and Mikusinski, 2014; Son et al., 2016; Li and Zhang, 2017). Even in Japan, a giant tree is symbolic of nature and has long been a home of various creatures, an object of worship, and a symbol of the local community (The Japanese Ministry of the Environment, 2017). Whereas old-growth giant trees might have faced an increased risk of death and falling because of aging, disease and external pressures such as typhoons. Climate change might accelerate damage to the growing conditions of old-growth giant trees through heavy rains, strong winds, and an increase in typhoons. Since some old-growth giant trees are located in temples and shrines close to the residential area, they might take a devastating toll on the livelihood of the people when falling (Kuroda et al., 2021; Hirano et al., 2021). Therefore, it is important to record the shape and size of old-growth giant trees both for the sake of documenting a valuable resource and for observing the condition of the trees.

In order to record and measure the shape of old-growth giant trees, it is necessary to be able to obtain data on the whole large tree. Recently, terrestrial laser scanning (TLS) and backpack personal laser scanning (BPLS) has used as a method to capture the whole shape of trees (Disney M. et al., 2019; Lecigne et al., 2021). TLS and BPLS obtain high-density point clouds and can get more detailed information on forest internal structure, including tree location, DBH, tree height, crown width, and other biophysical parameters (Bazezew et al., 2018; Liang et al., 2019; Wang et al., 2019; Yrttimaa et al., 2019). However, the equipment is expensive and professional to the public. The cooperation of

local citizen volunteers is essential to record and maintain the old-growth giant trees since about 70,000 old-growth giant trees and forests have been registered in Japan (The Japanese Ministry of the Environment, 2017). In fact, most registered trees were recorded by local citizen volunteers. An inexpensive and easy-to-use equipment that can be used by local citizen volunteers is required. Furthermore, TLS and BPLS cannot obtain images to identify the conditions of old-growth giant tree by the color of leaves and trunks (Sankaran et al., 2010; Metzger et al., 2004).

In recent years, UAVs have become smaller and cheaper, and more and more familiar to citizens. Several studies have recorded and measured medium-to-small-sized trees using UAV and SfM (Structure from Motion) technology. Scher et al. (2019) examined drone-based photogrammetry for the construction of high-resolution models of individual trees. They found that the models captured diameter and interior internode length of branches well for an American elm (*Ulmus americana* cultivar 'New Horizon') and a black walnut (*Juglans nigra*). Moreira et al. (2021) reported the combination of UAV images and SfM could measure the DBH of individual trees, which were olives with approximately 5 m tall, with very good accuracy under well-designed methodologies. Although there are few studies on old-growth giant trees, UAVs that can fly at high altitudes would be suitable to obtain data on old-growth giant trees.

The purpose of this study was to record and measure the shape and size of old-growth giant trees as valuable resources using UAVs which are inexpensive and easy-to-use equipments and can fly at high altitudes.

## 2. Materials and Methods

Fig. 1 shows the procedure of this study.

### 2.1 Sites and focal trees

#### 2.1.1 Japanese larch and Japanese cedar in Mie University Forest

Two open-grown trees of different species, which are a Japanese larch (Fig. 4, *Larix kaempferi*) and a Japanese cedar (Fig. 5, *Cryptomeria japonica*), were chosen within the grounds of Mie University Forest, Mie prefecture, Central Japan (Fig. 2, 34° 27' 32", 136° 14' 15") at an elevation of 672 m and 523 m above sea level. The mean annual precipitation is 2,481.9 mm yr<sup>-1</sup> and mean annual temperature is 12.3°C (for 1966-1995; Mie University Forest, 1998). These are not known when they were planted.

Japanese larch (*Larix kaempferi*) is one of the major plantation species in northern and central regions of Japan (Kurinobu 2005). This larch is a tall deciduous coniferous tree with a height of up to 30 m and a diameter at breast height of about 1 m. Its bark is dark brown, sometimes red, and peels off in thin scales. Tree crown shapes are usually slightly elongated cones (Yano, 1994).

Japanese cedar (*Cryptomeria japonica*) is a coniferous tree native to Japan, distributed in northern Honshu, Shikoku, Kyushu, and Yaku Island, although there are some planted in southern Hokkaido and Taiwan. This cedar is a large, straight-trunked tree with a height of 40-60 m and a diameter of 2-6 m at the breast height. The bark is reddish brown or grayish brown, fibrous, and peels longitudinally. The tree crown forms a conical to ovate canopy (Takakuwa, 2012).

### **2.1.2 Old-growth and giant Japanese cedar in Mt. Nonobori**

An open-grown tree was chosen at Mt. Nonobori in Kameyama city, Mie Prefecture (Fig. 3, 34° 56' 46", 136° 24' 59"), which is a Japanese cedar (Fig. 6, *Cryptomeria japonica*) at an elevation of 846 m above sea level. The mean annual precipitation is 1,853.7 mm yr<sup>-1</sup> and mean annual temperature is 15.1°C (Kameyama city at 70m, for 1991-2020; Japan Meteorological Agency). This tree is registered in the list of Giant Trees and Big Trees Forest Database as old-growth and giant trees (The Japanese Ministry of the Environment, 2022). Although the actual age of the tree is unknown, it is said to be over 300 years old. There were about 100 old-growth giant Japanese cedar trees in this area, making it a veritable forest of giant trees. However, the typhoon in 1998 caused great damage to the giant tree forest, and many trees were broken or uprooted (The Japanese Ministry of the Environment, 1998).

Japanese cedar (*Cryptomeria japonica*) is a coniferous tree native to Japan, distributed in northern Honshu, Shikoku, Kyushu, and Yaku Island, although there are some planted in southern Hokkaido and Taiwan. This cedar is a large, straight-trunked tree with a height of 40-60 m and a diameter of 2-6 m at the breast height. The bark is reddish brown or grayish brown, fibrous, and peels longitudinally. The tree crown forms a conical to ovate canopy (Takakuwa, 2012).

## **2.2 Photo capture**

### **2.2.1 TELLO**

In order to capture photos of the Japanese larch in Mie University Forest, and the Japanese cedar in Mt. Nonobori, TELLO/DJI (China) was used. TELLO is a mini drone quadcopter with a take-off weight of 80 g and dimensions of 98 mm L × 92.5 mm W × 41 mm H. The drone is equipped with

an RGB camera (Table 1). As all take-off and landings were performed manually, the drone was equipped with a propeller protection to ensure operator safety.

### **2.2.2 BLUEGRASS FIELDS**

In order to capture photos of the Japanese cedar in Mie University Forest, BLUEGRASS FIELDS/Parrot (France) was used. BLUEGRASS FIELDS is a quadcopter drone with a take-off weight of 1850 g and dimensions of 500 mm L × 440 mm W × 120 mm H. The drone was equipped with a Sequoia Multispectral sensor and a full HD video camera (Table 2). In this study, only the video camera is used to collect vertical aerial images.

### **2.2.3 Flight in Mie University Forest**

The UAV (TELLO) was designed to fly vertically around the Japanese larch (Fig. 7 a). Two concentric circles were laid out for the focal tree at a distance where the entire tree was able to be captured which were 6 m and 10 m. Takeoff positions were set in 22.5-degree increments in all directions on the concentric circle, except for directions with obstacles, with a total of four directions. UAV images were taken from these four directions vertically with the camera facing toward the focal trees. The lowest position where the image was taken was 1-2 m above the ground, and each position was 1 m above the last, continuing until the highest position was 1-2 m above the top of the tree. Several 1 to 2 m long poles were placed near the foot of the tree as markers to be used to scale the model (Fig. 7 b). UAV images were taken on 21st June 2021 between 12:00 and 14:00 (JST). There was a total of 100 images taken of this tree. All images had a photo resolution of 2592 × 1936 pixels.

The UAV (BLUEGRASS FIELDS) was designed to fly vertically around the Japanese cedar (Fig. 8 a). Two concentric circles were laid out for the focal tree at a distance where the entire tree was able to be captured, which were 7 m/8 m and 10 m. Takeoff positions were set in 30-degree increments in all directions on the concentric circle, except for directions with obstacles, with a total of six directions. UAV images were taken from these six directions vertically with the camera facing toward the focal trees. The lowest position where the image was taken was 1-2 m above the ground, and each position was 1 m above the last, continuing until the highest position was 1-2 m above the top of the tree. Several 1 m to 2 m long poles were placed near the foot of the tree as markers to be used to scale the model (Fig. 8 b). UAV images were taken on 19th November 2021 between 13:00 and 15:00 (JST). There was a total of 387 images taken for this tree. All images had a photo resolution of 4096 × 3072 pixels.

#### **2.2.4 Flight in Mt. Nonobori**

The UAV (TELLO) was designed to fly vertically around the Japanese cedar (Fig. 9 a). One concentric circle was laid out for the focal tree at a distance where the entire tree was able to be captured which was 13-14 m. Takeoff positions were set in about 90-degree increments in all directions on the concentric circle, with a total of four directions. UAV images were taken from these four directions vertically with the camera facing toward the focal trees. The lowest position where the image was taken was 1-2 m above the ground, and each position was 1 m above the last, continuing until the highest position was 1-2 m above the top of the tree. Several 1 m to 2 m long poles were placed near the foot of the tree as markers to be used to scale the model (Fig. 9 b). UAV images were taken

on 25th April 2022 between 12:00 and 14:00 (JST). There was a total of 93 images taken for this tree.

All images had a photo resolution of  $2592 \times 1936$  pixels.

### **2.3 Photo processing**

Agisoft Metashape Professional Edition 1.7.1 (Agisoft/Russia) which is a 3D modelling software was used for UAV photogrammetric processing. Metashape offers a user-friendly workflow that combines proprietary algorithms based on computer vision SfM and stereo-matching for image alignment and reconstruction of the 3D image (Verhoeven et al., 2012). The workflow included image alignment, building a dense point cloud (Dense Cloud), building mesh, building orthomosaic, building texture and building 3D model. During the image alignment stage, the stage at which camera location, orientation and other internal parameters are optimized (Agisoft, 2018), we used medium accuracy for image matching. Using the SfM techniques, this stage extract features within the images and match those features to pair the images. This stage produced a sparse 3D point cloud. After initial alignment, we deleted many extraneous points based on gradual selection procedures in Metashape (Agisoft, 2018) to speed up the dense cloud reconstruction process and for more accurate points. We then added markers in each corresponding image for a more accurate optimization of camera positions and orientation as well as other internal camera parameters. In the building dense point cloud stage, the stage that generates a dense point cloud, we used high quality to generate more points and mild depth filtering to remove the outliers. We followed the Metashape default setting for the 3D building stage and orthomosaic building stage (Fig.10).

For the Japanese larch in Mie University Forest, 4,541,024 points were generated in the dense point cloud, while the Japanese cedar generated 19,144,068 points. Orthophotos were generated from four directions for Japanese larch, and Japanese cedar generates orthophotos from six directions. The orthophotos had an average ground sample distance of 0.42 cm/pix for the Japanese larch, and 0.59 cm/pix for the Japanese cedar.

For the Japanese cedar in Mt. Nonobori, 3,188,978 points were generated and the orthophotos were generated from four directions with an average ground sample distance of 0.59 cm/pix.

## **2.4 Validating accuracy**

### **2.4.1 Tree heights and DBHs obtained from orthophotos, dense clouds and 3D models**

Tree heights and DBHs were measured using the ruler tool in Metashape.

For the measurements in orthophotos, tree heights and DBHs were measured planarly from the sides in the directions in which the orthophotos were generated (Fig. 11). For the measurements in dense clouds and 3D models (Fig. 12 and 13), the tree height was measured by carefully rotating the model to find the apex and measuring the distance of straight lines which from that point to the ground. DBH was calculated from the longest and shortest diameters inside the tree trunk measured at 1.3 m from the ground. The shortest diameter was a line drawn perpendicular to the longest diameter.

The approximate circle of the tree trunk at 1.3 m from the ground was also used to estimate the DBH as a reference and comparison of the DBHs in the dense cloud and the 3D model (Fig. 14).

### **2.4.2 Ground Data Acquisition**

All the trees analyzed in this study had their tree heights and trunk circumferences manually quantified with Vertex IV (Haglöf Sweden AB, Sweden) and a tape measure, respectively, to compare the ground truth values to the remote estimations for accuracy assessment. The height typically used for trunk circumference measurements is close to 1.3 m (Wieser et al., 2017). Tree height measurements were carried out one or two times from different directions, and average height values were assumed as the corresponding tree height. DBH was calculated from trunk circumferences. These surveys were conducted on the same day as the UAV filming.

### **2.4.3 Data Analysis**

We compared the tree heights and DBHs of all the individual trees. That is, tree heights from field ground survey vs. tree heights from orthophotos, dense clouds and 3D models, DBHs from field ground survey vs. DBHs from orthophotos, dense clouds and 3D models.

### **3. Results**

#### **3.1 Japanese larch and cedar in Mie University Forest**

##### **3.1.1 Orthophotos, Dense Cloud, 3D Model of the Japanese larch**

Figure 15-17 show the generated orthophotos, dense cloud and 3D model of the Japanese larch in Mie University Forest. Four orthophotos from four sides were generated using 29, 30, 29 and 28 photos respectively. For the dense cloud and 3D model, 100 photos were used. The image quality of the Japanese larch used for generating dense cloud and 3D model was calculated by the quality estimation function in Metashape for all 100 successfully aligned images in all 116 photos, and the average image quality value was 0.85.

The treetop is important to be clearly visible in order to measure tree heights. Although there are some parts that were not well reconstructed because of the neighboring tree, all orthophotos were able to reconstruct the tree trunk in all four directions (Fig. 15). In total, 4,541,024 points were generated for dense cloud. More than half of the tree shape in the vertical direction was successfully reconstructed in the dense cloud and the 3D model. Even though the other half of the tree was not successfully reconstructed because of the overlap with a neighboring tree, the parts where tree height and DBH could be measured were well reconstructed (Figs. 16 and 17).

##### **3.1.2 Tree heights and DBHs of the Japanese larch**

Table 3, Fig. 18 and 19 show tree heights obtained from the ground, orthophotos, dense cloud and 3D model. Since we couldn't stay far enough from the target tree, the directions in which the treetop was visible from the ground were restricted. Therefore, tree heights were measured from only two directions (Direction 1 and 2) using Vertex. The tree heights measured from the ground were 21.8

m and 25.8 m (average: 23.80 m). In orthophotos, dense cloud and 3D model, tree heights measured from the four directions were 17.5-20.3 m (average: 19.19 m), 19.6-19.9 m (average: 19.75 m) and 19.6-19.9 m (average: 19.75 m), respectively (Table 3). In Direction 1 and 2, tree heights measured from the ground were about 2-6 m higher than the reconstructions, and on average it was about 4 m higher than the reconstructions (Fig. 18 and 19).

Table 4, Fig. 20 and 21 show DBHs obtained from the ground, orthophotos, dense cloud and 3D model. DBH calculated from the ground result measured with a tape measure was 51.91 cm. DBHs measured in the orthophotos were 47.0-52.0 cm from four directions (average: 48.83 cm). DBHs in dense cloud and 3D model calculated from the longest and shortest diameters were 47.5 and 53.0 cm (average: 50.25 cm), 50.5 and 55.0 cm (average: 52.75 cm), respectively. While the DBHs estimated from the approximate circles in dense cloud and 3D model were 51.33 and 54.03 cm, respectively (Table 4). Compared with the DBH obtained from the ground, the difference with the average DBH of each reconstruction measured from different directions was -3.08 to +0.84 cm, and the difference with the estimated DBHs from the approximate circles in dense cloud and 3D model were -0.58 and -2.12 cm (Fig. 20 and 21).

### **3.1.3 Orthophotos, Dense Cloud, 3D Model of the Japanese cedar**

Figure 22-24 show the generated orthophotos, dense cloud and 3D model of the Japanese cedar in Mie University Forest. Six orthophotos from six sides were generated using 29, 65, 65, 68, 63 and 31 photos respectively. For dense cloud and 3D model, 321 photos were used. The image quality of the Japanese cedar which used for generating dense cloud and 3D model was calculated by the quality

estimation function in Metashape for all 321 successfully aligned images in all 387 photos, and the average image quality value was 0.71.

The treetop is important to be clearly visible to measure tree heights. Although there are some parts that were not well reconstructed because of the lack of the UAV images, orthophotos were able to reconstruct the tree trunk and treetop in all six directions (Fig. 22). Dense cloud was generated with 19,144,068 points. Although almost the entire tree shape was successfully reconstructed, there was a small part of the tree that wasn't reconstructed due to lack of the UAV images. Several branches from neighboring trees prevented the UAV from flying in certain directions. However, in the dense cloud and the 3D model, the part where tree height and DBH could be measured were well reconstructed (Fig. 23 and 24).

### **3.1.4 Tree heights and DBHs of the Japanese cedar**

Table 5, Fig. 25 and Fig. 26 show tree heights obtained from the ground, orthophotos, dense cloud and 3D model. Since we couldn't stay far enough from the target tree, the directions in which the treetop was visible from the ground were restricted. Therefore, only two directions (Direction 2 and 5) were used to measure tree heights with Vertex. The tree heights measured from the ground were 38.0 and 42.9 m (average: 40.45 m). In orthophotos, dense cloud and 3D model, tree heights measured from six directions were 33.7-35.9 m (average: 34.65 m), 36.2-36.5 m (average: 36.36 m) and 35.6-35.7 m (average: 35.64 m), respectively (Table 5). In Direction 2 and 5, tree heights measured from the ground were about 2-8 m higher than the reconstructions, and on average it was about 4-6 m higher than the reconstructions (Fig. 25 and 26).

Table 6, Fig. 27 and Fig. 28 show DBHs obtained from the ground survey, orthophotos, dense cloud and 3D model. DBH calculated from the ground measured with a tape measure was 126.91 cm. DBHs measured in the orthophotos were 124.0-134.7 cm (average: 129.83 cm) from six directions. DBHs in dense cloud and 3D model calculated from the longest and shortest diameters were 128.3-137.7 cm (average: 133.00 cm), 130.7-139.0 cm (average: 134.84 cm), respectively. While the DBHs estimated from the approximate circles in dense cloud and 3D model were 140.64 and 142.55 cm, respectively (Table 6). Compared with the DBH obtained from the ground, the difference with the average DBH of each reconstruction measured from different directions was +2.92 to +7.92 cm, and the difference with the estimated DBHs from the approximate circles in dense cloud and 3D model were +13.73 and +15.64 cm (Fig. 27 and 28).

### **3.2 Old-growth giant Japanese cedar in Mt. Nonobori**

#### **3.2.1 Orthophotos, Dense Cloud, 3D Model**

Figure 29-31 show the generated orthophotos, dense cloud and 3D model of Japanese cedar in Mt. Nonobori. Four orthophotos from four sides were generated using 26, 30, 9 and 28 photos respectively. For dense cloud and 3D model, 65 photos were used. The image quality of the Japanese cedar which used for generating dense cloud and 3D model was calculated by the quality estimation function in Metashape for all 65 successfully aligned images in all 93 photos, and the average image quality value was 0.85.

The treetop is important to be clearly visible in order to measure tree heights. Although there are some parts that were not well reconstructed because of the influence of light and shadow conditions,

orthophotos were able to reconstruct the tree trunk in all four directions, and the treetop in three directions (Fig. 29). Dense cloud was generated with 3,188,978 points. More than half of the tree shape in the vertical direction was successfully reconstructed in the dense cloud. Although the other half of the tree was not successfully reconstructed because of the light and shadow conditions, the part where tree height and DBH could be measured were well reconstructed (Fig. 30 and 31).

### 3.2.2 Tree heights and DBHs

Table 7, Fig. 32, and Fig 33 show tree heights obtained from the ground, orthophotos, dense cloud and 3D model. Since we couldn't have distance from the target tree enough, the directions in which the treetop was visible from the ground were restricted. Therefore, only two directions (Direction 1 and 3) were used to measure tree heights using Vertex, and they were 30.1 and 36.9 m (average: 33.50 m). In orthophotos, dense cloud and 3D model, tree heights measured from two directions were 28.6 and 29.8 m (average: 29.20 m), 30.2-30.7 m (average: 30.40 m) and 30.3-30.8 m (average: 30.54 m), respectively (Table 7). In Directions 1 and 3, compared with the average tree height measured from the ground, the difference with the average of each reconstruction was -2.96 to -4.30 m (Fig. 32 and 33). Orthophotos could not be reconstructed in those directions and are excluded from this comparison by directions.

Table 8, Fig. 34 and Fig 35 show DBHs obtained from the ground, orthophotos, dense cloud and 3D model. The DBH calculated from the ground measured with a tape measure were 161.46 cm. DBHs measured in orthophotos were 150.5-164.0 cm from two directions (average: 155.83 cm). DBHs in dense cloud and 3D model calculated from the longest and shortest diameters were 153.8

and 167.7 cm (average: 160.71 cm), 152.5 and 168.0cm (average: 160.25 cm), respectively. While the DBHs estimated from the approximate circles in dense cloud and 3D model were 164.85 and 169.27 cm, respectively (Table 8). Compared with the DBH obtained from the ground, and the difference with the average DBH of each reconstruction measured from different directions was -5.63 to -0.76 cm, and the difference with the estimated DBHs from the approximate circles in dense cloud and 3D model were +3.39 and +7.81 cm (Fig. 34 and 35).

## **4. Discussion**

### **4.1 Characteristics of tree heights and DBHs by measurement methods**

It was found through this study that we might be able to provide the method to obtain multi-directional and three-dimensional records of old-growth giant trees using UAV as a remote method. The difference between the DBHs estimated by the approximate circle method and the common ground-based method was -2.12 to +15.64 cm. While the difference between the common ground-based method and our measurements in different directions in the remote method was approximately 3-7 m in tree heights and 0-12 cm in DBHs.

In the tree height, the remote method in this study was always smaller than the ground-based method. It is known that the measurement of tree height from ground using triangulation methods such as Vertex has errors of 1-5 m or more, largely due to the limited visibility of the very top of the tree from the ground (Bragg, 2008; Goetz et.al., 2011). Moreover, Larjavaara and Muller-Landau (2013) indicated that due to the difficulty in determining the exact locations of the base and the top of the tree from a distance, operators tend to shoot high up when using tangential tree height instruments, leading to overestimation of the tree height. Our results show the same tendency. The measurement using orthophotos might not have been able to capture the true treetops same as ground-based method as heights were measured from each lateral view. Although the deviation within the same method was less than 0.5 m in the dense cloud and 3D model, it was about 1-3 m in the orthophotos. Measurement differences are likely to be small due to nearly identical treetops being able to capture measurements in all directions in dense clouds and 3D models by rotating the model.

In the DBH measurement, although the DBH varied depending on the direction of measurement since the trunk is not perfectly round, we could not find any tendency in the difference. The difference between measured values might have been due to the methods. Namely, on the ground, the circumference of tree trunks was measured using a tape measure, and DBHs were calculated. In the orthophoto, it measured the width of the tree trunk from each lateral view. While DBHs in dense clouds and 3D models were measured and estimated by two different methods. One was to measure the longest and shortest diameters and take the average of the two as the DBH. The other was to estimate by the approximate circle.

Recently, the terrestrial laser scanning (TLS) and backpack personal laser scanning (BPLS) has used as a method to capture the whole shape of trees (Disney, 2019; Lecigne et al., 2021). TLS and BPLS obtain high density point clouds and can get more detailed information on forest internal structure, including tree location, DBH, tree height, crown width, and other biophysical parameters (Bazezew et al., 2018; Liang et al., 2019; Wang et al., 2019; Yrttimaa et al., 2019). By using TLS and BPLS, it has been reported that tree height and DBH can be measured with an accuracy of -9.90 m to +3.06 m, and -1.11 cm to +1.71 cm, respectively (Table 9). The results in this study showed similar differences in tree height with theirs, while the difference in DBH were larger than them. Some studies estimated DBHs based on circumferences approximating the cross-section of the trunk, the value would be more similar to the ground-based method than our methods that measured from different directions. However, the DBHs estimated from the approximate circles in this study show a more significant difference, especially when trees have bigger trunks. DBHs of trees in other studies were less than 100 cm, and the DBHs of the Japanese larch in this study (DBH<100 cm) show similar

accuracy (-2.12 to -0.58 cm). In addition, Zhang, Y. et al. (2022) indicated that image quality as one of the important parameters in Metashape software would affect 3D recovery. In this study, image quality of the Japanese cedar in the Mie University Forest (image quality: 0.71) was not as good as the other two (image quality: 0.85, 0.85), which might significantly affect the reconstruction, bringing up more noise points. The results might be improved with a better camera. Furthermore, the advantage of UAV data collection compared to TLS and BPLS are the ability to acquire images to identify the condition of the old-growth giant trees through the color of leaves and trunks.

#### **4.2 Environments of data acquisition**

We designed the flight path to take images from different directions in two concentric circles to obtain detailed images of the target trees (Scher et al., 2019) except for the Japanese cedar in Mt. Nonobori. In Mt. Nonobori, it was taken from different directions in one concentric circle. When there are trees or buildings around the target tree, there might not be enough space for the UAV to fly. At this case, we might need to reduce the number of concentric circles or increase the interval between shooting directions, but we also need to consider whether the images taken under such a flight path can provide us with sufficient results. Although it is not caused by only it, orthophoto, dense cloud and 3D model were not enough reconstructed in the Japanese cedar in Mt. Nonobori.

In this study, there were some missing parts under some branches and leaves in the dense cloud and 3D model, especially when the crown size of the target tree was larger. We might need to change the camera angle depending on objects. During the images taking of the target trees, we left the camera angle at the default setting which was horizontal (0°). Moreira et al. (2021) proposed a way to

complement it by adjusting camera's shooting angle. They varied the tilt of the camera from vertical (90°, nadir) to oblique (60°) in order to obtain viewpoints of tree trunks completely or partially hidden under the canopies during the acquisition of images using the UAV. It helped to reconstruct the parts under the branches or leaves.

It is also necessary to devise light conditions. There were some parts of the trees could not be reconstructed in the dense cloud and 3D model caused by the difference between the shaded part of the trees and the part with strong light. Scher et al. (2019) evaluated the ambient light conditions in the drone-based photogrammetry method and pointed out that the models reconstructed using images taken on sunny days had larger errors than those using images taken on overcast day. It was reported that the occurrence of shadows and uneven illumination can also affect the quality of the point cloud (Dandois et al., 2015). Although there is no option to remove the trees and buildings around the target trees, we would consider and decide the weather and time of day for taking images.

#### **4.3 Benefit from citizen volunteers**

The cooperation of local citizen volunteers is essential to recording and maintaining the old-growth giant trees since about 70,000 old-growth giant trees and forests have been registered in Japan (The Japanese Ministry of the Environment, 2017). In fact, most registered and measured trees were recorded by local citizen volunteers. Since they are rarely equipped with specialist and expensive equipment such as Vertex, tree height is usually measured visually, and trunk circumference is measured with a tape measure. In addition, since old-growth giant trees often has an intricate and unique shape, it is difficult to describe their appearance through these measurements accurately.

Therefore, it is recommended to make sketches and take photos of the trees (Biodiversity Center of Japan, 2000). Although it might still be difficult for local citizen volunteers to generate orthophotos, dense clouds and 3D models because it requires specialized software and knowledge, it has become much easier to obtain images of target trees using UAV. In recent years, UAVs have become smaller and cheaper, making them more and more familiar to citizens. We used two types of UAVs in this study, one costs about 10,000 yen for TELLO and the other is about 600,000 yen for BLUEGRASS FIELDS. We found that we could obtain data even low-cost products was comparable to expensive one. Moreover, although the tallest tree is Japanese cedar (*Cryptomeria japonica*), which is 62.3 m in Japan (Forestry Agency, 2017), the maximum flight altitudes of many UAVs exceed these. We should start asking local citizen volunteers to regularly use drones to photograph trees and accumulate data. old-growth giant trees are facing the problem of aging and given their longevity and the pressures of environmental change, we need to start recording those trees immediately.

## **5. Conclusion**

Through our research, we found that we might be able to provide a method of using UAV as a remote method to obtain multi-directional and three-dimensional records of old-growth giant trees. Old-growth giant trees are facing the problem of aging and given their longevity and the pressures of environmental change, we need to start recording these trees immediately using UAV with the help of citizen volunteers.

## **Acknowledgment**

First and foremost, I am extremely grateful to my supervisors, Dr. Itaya for her invaluable advice, continuous support, and patience during my master study. Her immense knowledge and plentiful experience have encouraged me in all the time of my academic research and daily life. I would also like to thank Prof. Ishikawa, who always gave me support and advice in various ways. I would like to thank the staff in Mie University Forest for giving me support of my study. I would like to thank all the members in the Forest Engineering Lab. It is their kind help and support that have made my study and life in the Japan a wonderful time.

I would also like to extend my sincere thanks to Honda Benjiro Shogaku Kikin Scholarship, without which it would be difficult for me to concentrate on my study. Ultimately, I would like to express my deepest gratitude to my family in China, if it weren't for them, I wouldn't be where I am today.

## References

- Becker, N. and Freeman, S. (2009) The economic value of old growth trees in Israel. *Forest Policy and Economics*, 11(8), 608-615.
- Blicharska, M. and Mikusiński, G. (2014) Incorporating social and cultural significance of large old trees in conservation policy. *Conservation Biology*, 28(6), 1558-1567.
- Son, Hee-Jun, Xia, Tian-Tian, Kim, Young-Hun and Kang Tai-Ho (2016) A Value Evaluation Research of the Old-growth and Giant Tree - Focus on Gyeongju Gyerim's *Zelkova Serrata* -. *Journal of the Korean Institute of Traditional Landscape Architecture*, 34(4), 51–56.  
<https://doi.org/10.14700/KITLA.2016.34.4.051>.
- Li, Y. and Zhang, Q. B. (2017) History of tree growth declines recorded in old trees at two sacred sites in northern China. *Frontiers in Plant Science*, 8, 1779.
- The Japanese Ministry of the Environment (2017) Database of Giant Trees and Giant Forests: What is the Giant Tree and Giant Forest Survey?  
[https://kyoju.biodic.go.jp/?\\_action=gtother&\\_command=bigtreesurvey](https://kyoju.biodic.go.jp/?_action=gtother&_command=bigtreesurvey). (in Japanese)
- Kuroda Keiko, Taga Masaaki, Murao Mitsuru, Miyajima Hideyoshi and Mori Yasuo (2021) Cause of the collapse of a giant tree at Okute Shinmei Shrine in Gifu Prefecture and problems in managing old trees. *Japan Forest Society Conference Presentation Database* doi:  
[https://doi.org/10.11519/jfsc.132.0\\_32](https://doi.org/10.11519/jfsc.132.0_32). (in Japanese)
- Hirano Yasuhiro, Nanko Kazuki, Doi Ryuusei, Nishimura Rei, Iriyama Tetsuya and Tanikawa Toko (2021) Root system of the giant *Cryptomeria japonica* tree collapsed at Shinmei shrine in Okute town, Gifu, in July 2020. *Root Research* 30 (3): 65-75. (in Japanese)

- Disney, M., Burt, A., Calders, K., Schaaf, C. and Stovall, A. (2019) Innovations in ground and airborne technologies as reference and for training and validation: terrestrial laser scanning (TLS). *Surveys in Geophysics*, 40, 937-958.
- Lecigne, B., Delagrangé, S., and Taugourdeau, O. (2021) Annual shoot segmentation and physiological age classification from TLS data in trees with acrotonic growth. *Forests*, 12(4), 391.
- Bazewez, M. N., Hussin, Y. A. and Kloosterman, E. H. (2018) Integrating Airborne LiDAR and Terrestrial Laser Scanner forest parameters for accurate above-ground biomass/carbon estimation in Ayer Hitam tropical forest, Malaysia. *International Journal of Applied Earth Observation and Geoinformation*, 73, 638-652.
- Liang, X., Wang, Y., Pyörälä, J., Lehtomäki, M., Yu, X., Kaartinen, H., Kukko, A., Honkavaara, E., Issaoui, A. E. I., Nevalainen, O., Vaaja, M., Virtanen, J., Katoh, M. and Deng, S. (2019) Forest in situ observations using unmanned aerial vehicle as an alternative of terrestrial measurements. *Forest ecosystems* 6(1): 1-16.
- Wang Y., Lehtomäki M., Liang X., Pyörälä J., Kukko A., Jaakkola A., Liu J., Feng Z., Chen R., Hyypä J. (2019) Is field-measured tree height as reliable as believed – A comparison study of tree height estimates from field measurement, airborne laser scanning and terrestrial laser scanning in a boreal forest. *ISPRS Journal of Photogrammetry and Remote Sensing* 147: 132-145.

- Yrttimaa, T., Saarinen, N., Kankare, V., Liang, X., Hyypä, J., Holopainen, M., and Vastaranta, M. (2019) Investigating the feasibility of multi-scan terrestrial laser scanning to characterize tree communities in southern boreal forests. *Remote Sensing*, 11(12), 1423.
- Sankaran, S., Mishra, A., Ehsani, R. and Davis, C. (2010) A review of advanced techniques for detecting plant diseases. *Computers and electronics in agriculture*, 72(1), 1-13.
- Metzger, J. A., Storer, A. J. and Witter, J. A. (2004) Michigan ash monitoring plot system field methods protocol handbook. version 1.0. The Michigan Ash Monitoring Plot System: web page<  
<http://www.michiganash.org/publications.html>>.
- Zhang, Y., Onda, Y., Kato, H., Feng, B., and Gomi, T. (2022) Understory biomass measurement in a dense plantation forest based on drone-SfM data by a manual low-flying drone under the canopy. *Journal of Environmental Management*, 312, 114862.
- Scher, C. L., Griffoul, E. and Cannon, C. H. (2019) Drone-based photogrammetry for the construction of high-resolution models of individual trees. *Trees*, 33(5), 1385-1397.
- Moreira, B. M., Goyanes, G., Pina, P., Vassilev, O. and Heleno, S. (2021) Assessment of the influence of survey design and processing choices on the accuracy of tree diameter at breast height (DBH) measurements using UAV-based photogrammetry. *Drones*, 5(2), 43.
- Mie University Forest (1998) Climate of Mie University Forest. <https://hirakura.sakura.ne.jp/forests/catalog/wether/climate/>
- Kurinobu S. (2005) Forest tree breeding for Japanese larch. *Eurasian Journal of Forest Research*, 8(2), 127-134.

- Yano Makio (1994) Variation of the spherical fruit and its paleobotanical significance in "Japanese Larch", the northernmost tree in the Japanese Archipelago. *The Quaternary Research* 33(2): 95-105, <https://doi.org/10.4116/jaqua.33.95> (in Japanese)
- Takakuwa S. (2012) The connection between Japanese cedar and Japanese people. [accessed 2023 Jan 9]. [http://repo.kyoto-wu.ac.jp/dspace/bitstream/11173/1946/1/0160\\_025\\_008.pdf](http://repo.kyoto-wu.ac.jp/dspace/bitstream/11173/1946/1/0160_025_008.pdf) (in Japanese)
- Japan Meteorological Agency [accessed 2023 Jan 9] [https://www.data.jma.go.jp/obd/stats/etrn/view/nml\\_amd\\_ym.php?prec\\_no=53&block\\_no=0503&year=&month=&day=&view=](https://www.data.jma.go.jp/obd/stats/etrn/view/nml_amd_ym.php?prec_no=53&block_no=0503&year=&month=&day=&view=)
- The Japanese Ministry of the Environment (2022) Giant Trees and Big Trees Forest Database. [accessed 2023 Jan 9]. <https://kyoju.biodic.go.jp/>
- The Japanese Ministry of the Environment (1998) Biodiversity Center of Japan. [accessed 2023 Jan 9]. [https://www.biodic.go.jp/kiso/13/13\\_kyoju.html](https://www.biodic.go.jp/kiso/13/13_kyoju.html)
- Verhoeven, G., Doneus, M., Briese, C. and Vermeulen, F. (2012) Mapping by matching: a computer vision-based approach to fast and accurate georeferencing of archaeological aerial photographs. *Journal of Archaeological Science* 39(7): 2060-2070.
- Agisoft. LLC. (2018) Agisoft PhotoScan user manual: Professional edition, Version 1.4. [accessed 2023 Jan 9]. [https://www.agisoft.com/pdf/photoscan-pro\\_1\\_4\\_en.pdf](https://www.agisoft.com/pdf/photoscan-pro_1_4_en.pdf)
- Wieser, M., Mandlbürger, G., Hollaus, M., Otepka, J., Glira, P. and Pfeifer, N. (2017) A case study of UAS borne laser scanning for measurement of tree stem diameter. *Remote Sensing* 9(11): 1154.

- Bragg, D. C. (2008) An improved tree height measurement technique tested on mature southern pines. *Southern Journal of Applied Forestry*, 32(1), 38-43.
- Goetz, S. and Dubayah, R. (2011) Advances in remote sensing technology and implications for measuring and monitoring forest carbon stocks and change. *Carbon Management*, 2(3), 231-244
- Larjavaara, M. and Muller - Landau, H. C. (2013) Measuring tree height: a quantitative comparison of two common field methods in a moist tropical forest. *Methods in Ecology and Evolution*, 4(9), 793-801.
- Brolly G., Kiraly G. (2009) Algorithms for stem mapping by means of terrestrial laser scanning. *Acta Silv Et Lignaria Hungarica* 5:119–130
- Aruga K., Yanagihara E., Yamamoto T., Ishiguri F., Furusawa T., Akira K. (2017) Application of portable terrestrial laser scanner to a secondary broad-leaved forest. *Eur J for Eng* 3:7–15
- Yubo, L., Hongyu, H., Liyu, T., Chongcheng, C. and Hao, Z. (2019) Tree height and diameter extraction with 3D reconstruction in a forest based on TLS. *Remote Sensing Technology and Application*, 34(2), 243-252. (in Chinese)
- Furukawa S. and Nagashima K. (2020) The relationships between crown parameters, DBH, and tree volume measured from terrestrial laser scanner data. *Journal of Forest Planning* 54: 3-11 (In Japanese)
- Ko C., Lee S., Yim J., Kim D. and Kang J. (2021) Comparison of forest inventory methods at plot-level between a backpack personal laser scanning (BPLS) and conventional equipment in Jeju island. *South Korea for* 12:308

Maas HG., Bienert A., Scheller S. and Keane E. (2008) Automatic forest inventory parameter determination from terrestrial laser scanner data. *Int J Remote Sens* 29:1579–1593

Dandois, J. P., Olano, M. and Ellis, E. C. (2015) Optimal altitude, overlap, and weather conditions for computer vision UAV estimates of forest structure. *Remote Sensing*, 7(10), 13895-13920.

Biodiversity Center of Japan (2000) Basic measurement manual for giant trees and forests.

[https://www.biodic.go.jp/reports2/7th/7\\_kyojumanual/7\\_kyojumanual-1.pdf](https://www.biodic.go.jp/reports2/7th/7_kyojumanual/7_kyojumanual-1.pdf). (in Japanese)

Forestry Agency (2017) Japan's tallest cedar, Sanbon-sugi in Hanaseki (measurement results)

<https://www.rinya.maff.go.jp/kinki/kyoto/information/H29/291128sannbonsugi.html>

## **List of tables**

Table 1. Specification of UAV (TELLO/DJI)

Table 2. Specification of UAV (BLUEGRASS FIELDS/Parrot)

Table 3. Tree heights of the Japanese larch in Mie University Forest

Table 4. DBHs of the Japanese larch in Mie University Forest

Table 5. Tree heights of the Japanese cedar in Mie University Forest

Table 6. DBHs of the Japanese cedar in Mie University Forest

Table 7. Tree heights of the Japanese cedar in Mt. Nonobori

Table 8. DBHs of the Japanese cedar in Mt. Nonobori

Table 9. Accuracy of tree heights and DBHs measured by terrestrial laser scanning (TLS) and backpack personal laser scanning (BPLS) in previous studies

## **List of figures**

Fig 1. Methodological processes of this study.

Fig 2. Location of Mie University Forest.

Fig 3. Location of Mt.Nonobori.

Fig 4. Japanese larch in Mie University Forest.

Fig 5. Japanese cedar in Mie University Forest.

Fig 6. Japanese cedar in Mt.Nonobori.

Fig 7. Flying paths for the Japanese larch in Mie University Forest. a: UAV positions from the side.

b: UAV positions from the top.

Fig 8. Flying paths for the Japanese cedar in Mie University Forest. a: UAV positions from the side.

b: UAV positions from the top.

Fig 9. Flying paths for the Japanese cedar in Mt. Nonobori. a: UAV positions from the side. b: UAV

positions from the top.

Fig 10. Procedure of UAV images processing.

Fig 11. Measurement methods in the generated orthophotos.

Fig 12. Measurement methods in the generated dense cloud. a: Tree height measurement. b: DBH

measurement.

Fig 13. Measurement methods in the generated 3D model. a: Tree height measurement. b: DBH measurement.

Fig 14. Measurement method using approximate circle in the generated dense clouds and 3D models.

Fig 15. Orthophotos of the Japanese larch in Mie University Forest.

Fig 16. Dense Cloud of the Japanese larch in Mie University Forest.

Fig 17. 3D Model of the Japanese larch in Mie University Forest.

Fig 18. Tree heights of the Japanese larch in Mie University Forest.

Fig 19. Differ in the tree height measurements of the Japanese larch in Mie University Forest.

Fig 20. DBHs of the Japanese larch in Mie University Forest.

Fig 21. Differ in the DBH measurements of the Japanese larch in Mie University Forest.

Fig 22. Orthophotos of the Japanese cedar in Mie University Forest.

Fig 23. Dense Cloud of the Japanese cedar in Mie University Forest.

Fig 24. 3D Model of the Japanese cedar in Mie University Forest.

Fig 25. Tree heights of the Japanese cedar in Mie University Forest.

Fig 26. Differ in the tree height measurements of Japanese cedar in Mie University Forest.

Fig 27. DBHs of the Japanese cedar in Mie University Forest.

Fig 28. Differ in the DBH measurements of the Japanese cedar in Mie University Forest.

Fig 29. Orthophotos of the Japanese cedar in Mt.Nonobori.

Fig 30. Dense Cloud of the Japanese cedar in Mt.Nonobori.

Fig 31. 3D Model of the Japanese cedar in Mt.Nonobori.

Fig 32. Tree heights of the Japanese cedar in Mt.Nonobori.

Fig 33. Differ in the tree height measurements of the Japanese cedar in Mt.Nonobori.

Fig 34. DBHs of the Japanese cedar in Mt.Nonobori.

Fig 35. Differ in the DBH measurements of the Japanese cedar in Mt.Nonobori.

**Table 1. Specification of UAV (TELLO/DJI)**

	<b>Parameters</b>	<b>Specifications</b>
<b>Aircraft</b>	Speed	8m/s (maximum)
	Flight height	30m (maximum)
	Flight time	13min
	Size	98×92.5×41 mm
	Weight	80g
<b>Camera(RGB)</b>	Image resolution	5MP (2592x1936)

**Table 2. Specification of UAV (BLUEGRASS FIELDS/Parrot)**

	<b>Parameters</b>	<b>Specifications</b>
<b>Aircraft</b>	Speed	60km/h (maximum)
	Flight time	25mins (maximum)
	Size	50 x 44 x 12 cm
	Weight	1850g
<b>Video Camera</b>	Image resolution	14MP wide angle camera

**Table 3 Tree heights of the Japanese larch in Mie University Forest**

	Direction				Average
	1	2	3	4	
Vertex (m)	21.8	25.8	N/A	N/A	23.80
Orthophoto (m)	20.2	20.3	18.8	17.5	19.19
Dense Cloud (m)	19.9	19.6	19.7	19.8	19.75
3D Model (m)	19.9	19.6	19.7	19.9	19.75

**Table 4 DBHs of the Japanese larch in Mie University Forest**

	Direction				Average	Approximate circle
	1	2	3	4		
Tape (cm)		51.91			51.91	N/A
Orthophoto (cm)	52.0	47.0	47.0	49.3	48.83	N/A
Dense Cloud (cm)		Longest: 53.0; Shortest: 47.5			50.25	51.33
3D Model (cm)		Longest: 55.0; Shortest: 50.5			52.75	54.03

**Table 5 Tree heights of the Japanese cedar in Mie University Forest**

	Direction						Average
	1	2	3	4	5	6	
Vertex (m)	N/A	38.0	N/A	N/A	42.9	N/A	40.45
Orthophoto (m)	34.7	34.5	33.7	35.9	34.8	34.4	34.65
Dense Cloud (m)	36.5	36.2	36.3	36.3	36.4	36.5	36.36
3D Model (m)	35.7	35.6	35.6	35.6	35.6	35.7	35.64

**Table 6 DBHs of the Japanese cedar in Mie University Forest**

	Direction						Average	Approximate circle
	1	2	3	4	5	6		
Tape (cm)			126.91				126.91	N/A
Orthophoto (cm)	128.0	124.0	N/A	134.7	133.3	127.0	129.83	N/A
Dense Cloud (cm)		Longest: 137.7; Shortest: 128.3					133.00	140.64
3D Model (cm)		Longest: 139.0; Shortest: 130.7					134.84	142.55

**Table 7 Tree heights of the Japanese cedar in Mt. Nonobori**

	Direction				Average
	1	2	3	4	
Vertex (m)	30.1	N/A	36.9	N/A	33.50
Orthophoto (m)	N/A	29.8	N/A	28.6	29.20
Dense Cloud (m)	30.3	30.7	30.2	N/A	30.40
3D Model (m)	30.5	30.8	30.3	N/A	30.54

**Table 8 DBHs of the Japanese cedar in Mt. Nonobori**

	Direction					Average	Approximate circle
	1	2	3	4			
Tape (cm)		161.46				161.46	N/A
Orthophoto (cm)	N/A	164.0	N/A	150.5		155.83	N/A
Dense Cloud (cm)		Longest: 167.7; Shortest: 153.8				160.71	164.85
3D Model (cm)		Longest: 168.0; Shortest: 152.5				160.25	169.27

**Table 9 Accuracy of tree heights and DBHs measured by terrestrial laser scanning (TLS) and backpack personal laser scanning (BPLS) in previous studies**

<b>Difference of tree height between grand survey and TLS/BPLS</b>	<b>Tree species</b>	<b>Reference</b>
-9.90 ~ +2.28 m	<i>Quercus petraea, Carpinus betulus, Fagus sylvatica, Larix decidua, Picea abies</i>	Brolly & Kiraly (2009)
-1.02 ~ +1.45 m	<i>Quercus serrata, Magnolia obovate, Castanea crenata, Cerasus jama- sakura</i>	Aruga et al. (2017)
0 ~ 3.06 m	<i>Schima superba</i> and <i>Agathis</i>	Yubo et al. (2019)
+0.78 ~ +1.01 m	Japanese cypress ( <i>Chamaecyparis obtusa</i> )	Furukawa and Nagashima (2020)
-1.61 ~ -1.18 m	Japanese cedar ( <i>Cryptomeria Japonica</i> )	Ko et al. (2021)
<b>Difference of DBH between grand survey and TLS/BPLS</b>	<b>Tree species</b>	<b>Reference</b>
-0.67 ~ +1.58 cm	Spruce, Beech, Fir Spruce, Larch, Fir	Maas et al. (2008)
-0.18 ~ +0.76 cm	Pine, Spruce, Deciduous, Spruce	Liang and Hyypä (2013)
-1.11 ~ +0.39 cm	<i>Quercus serrata, Magnolia obovate, Castanea crenata, Cerasus jama- sakura</i>	Aruga et al. (2017)
0 ~ 1.71 cm	<i>Schima superba</i> and <i>Agathis</i>	Yubo et al. (2019)
-1.06 ~ -0.87 cm	Japanese cedar ( <i>Cryptomeria Japonica</i> )	Ko et al. (2021)

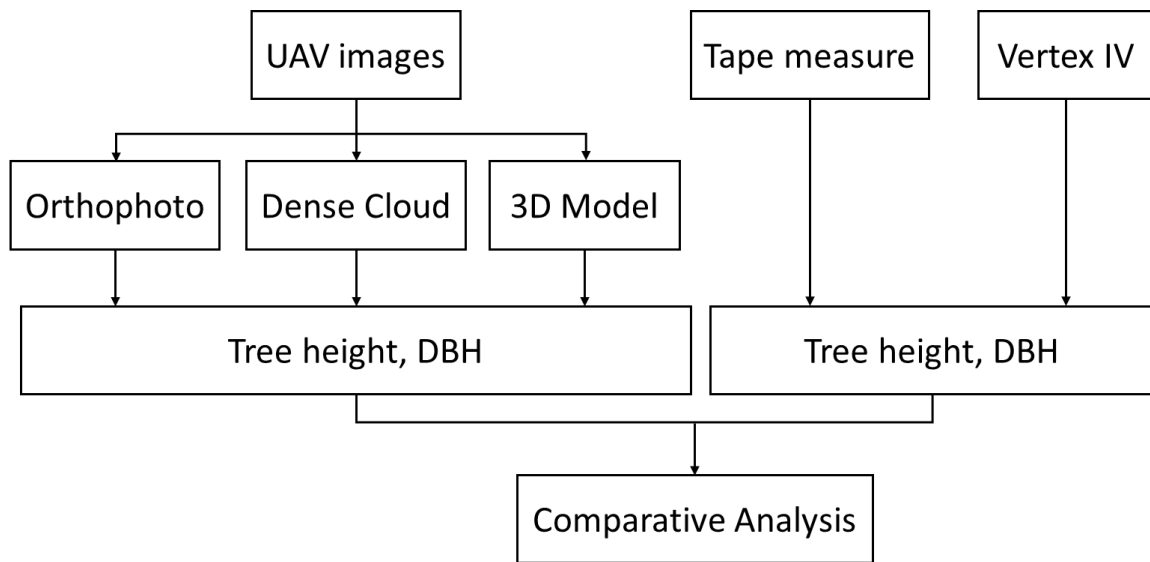


**Fig 1. Methodological processes of this study.**

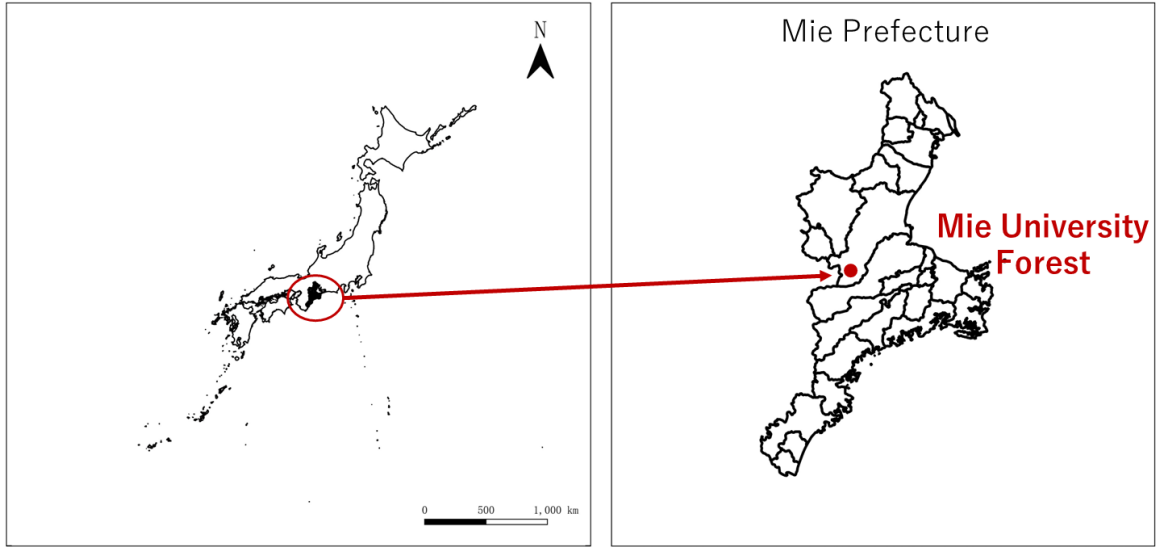


**Fig 2. Location of Mie University Forest.**

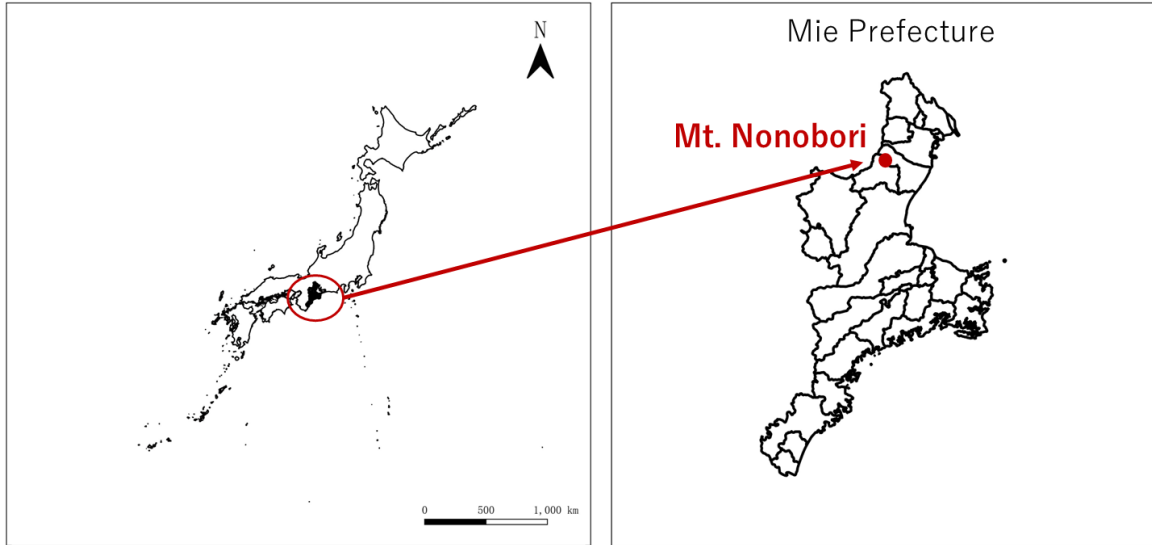


**Fig 3. Location of Mt.Nonobori.**



**Fig 4. Japanese larch in Mie University Forest.**



**Fig 5. Japanese cedar in Mie University Forest.**



**Fig 6. Japanese cedar in Mt.Nonobori.**

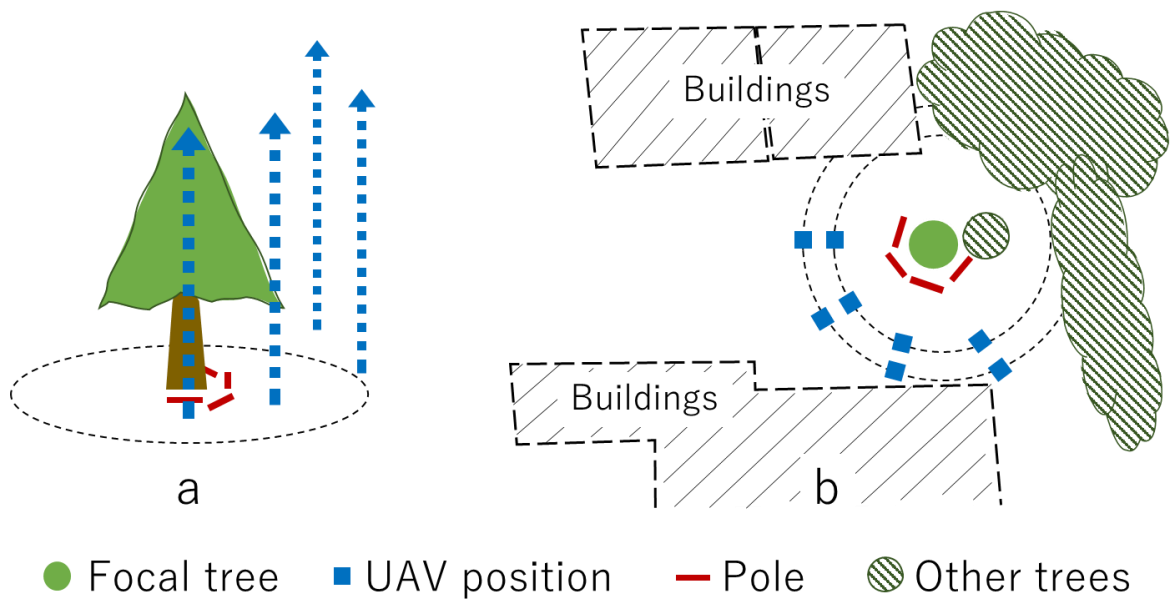


**Fig 7. Flying paths for the Japanese larch in Mie University Forest.**  
**a: UAV positions from the side. b: UAV positions from the top.**

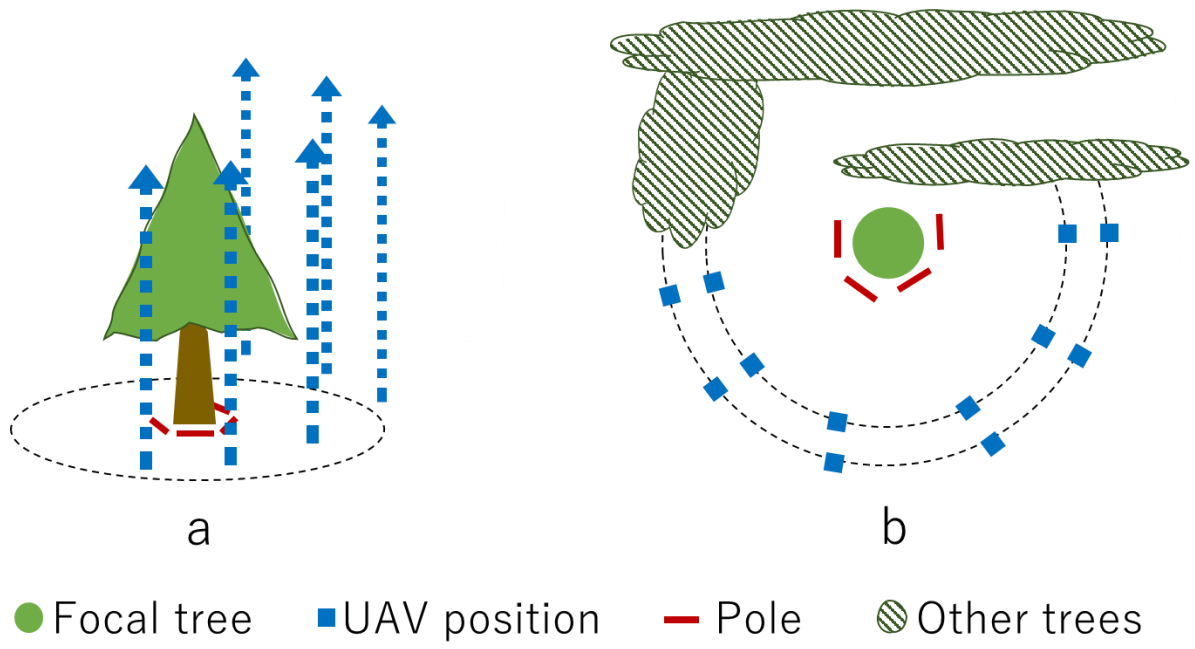


**Fig 8. Flying paths for the Japanese cedar in Mie University Forest.**  
**a: UAV positions from the side. b: UAV positions from the top.**

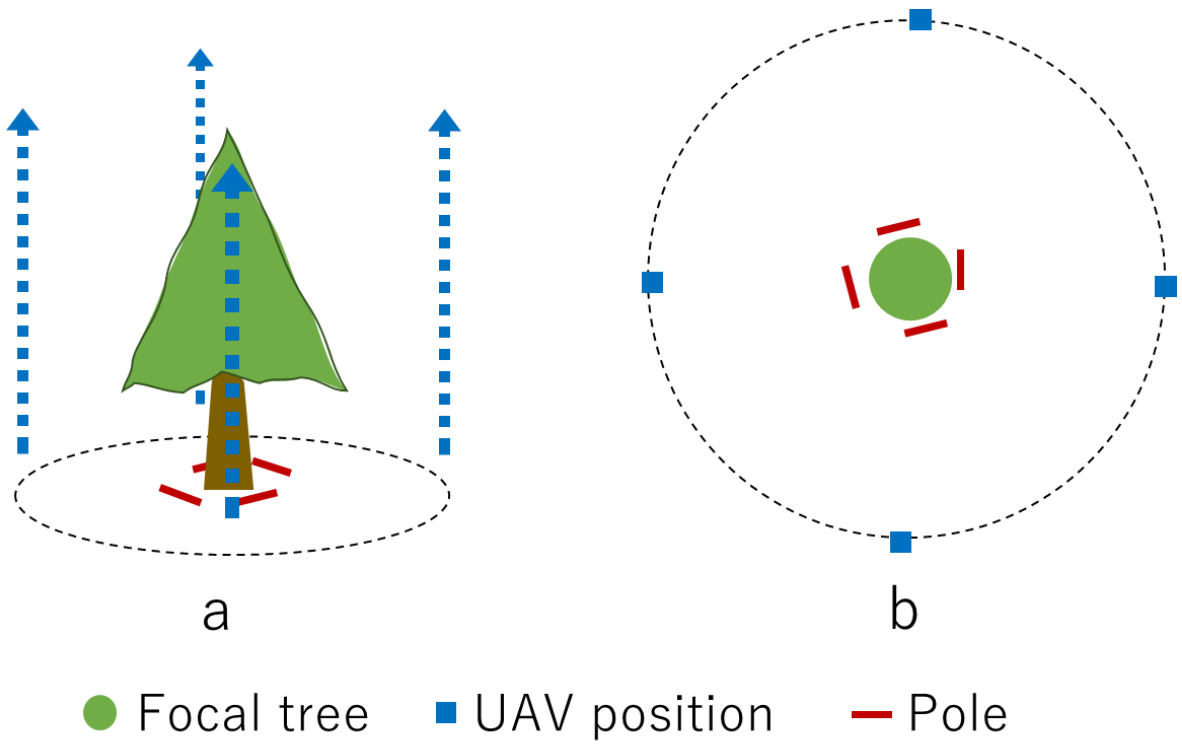


**Fig 9. Flying paths for the Japanese cedar in Mt. Nonobori.**  
**a: UAV positions from the side. b: UAV positions from the top.**

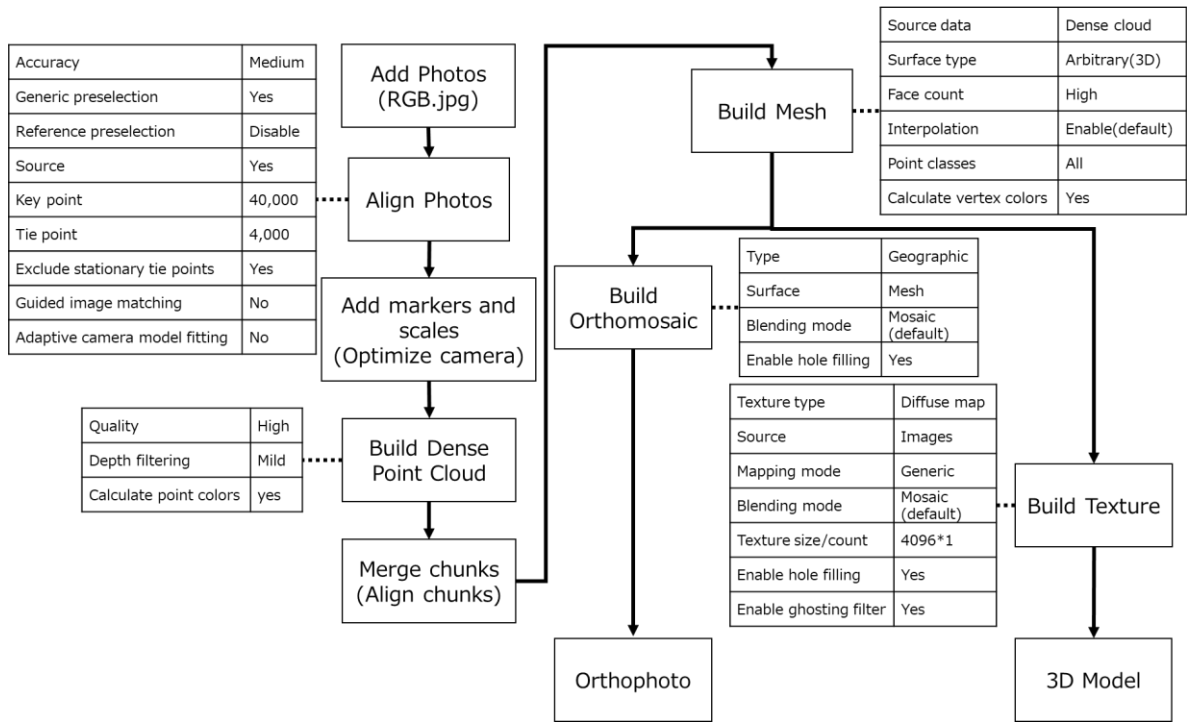


**Fig 10. Procedure of UAV images processing.**

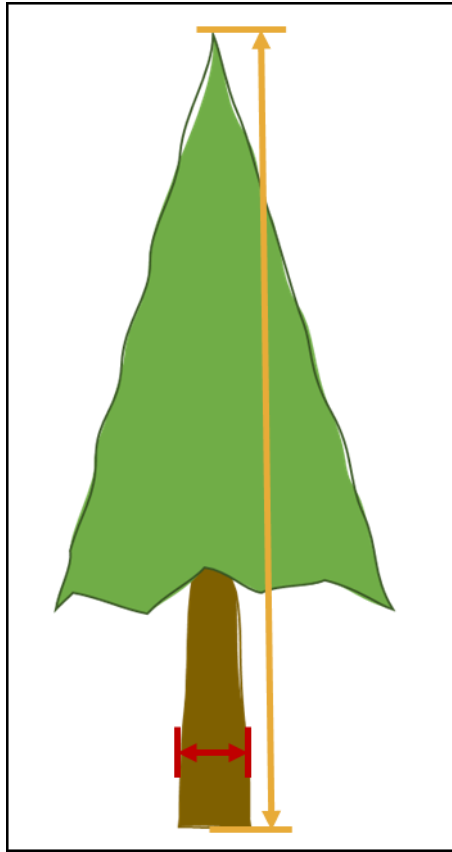


**Fig 11. Measurement methods in the generated orthophotos.**

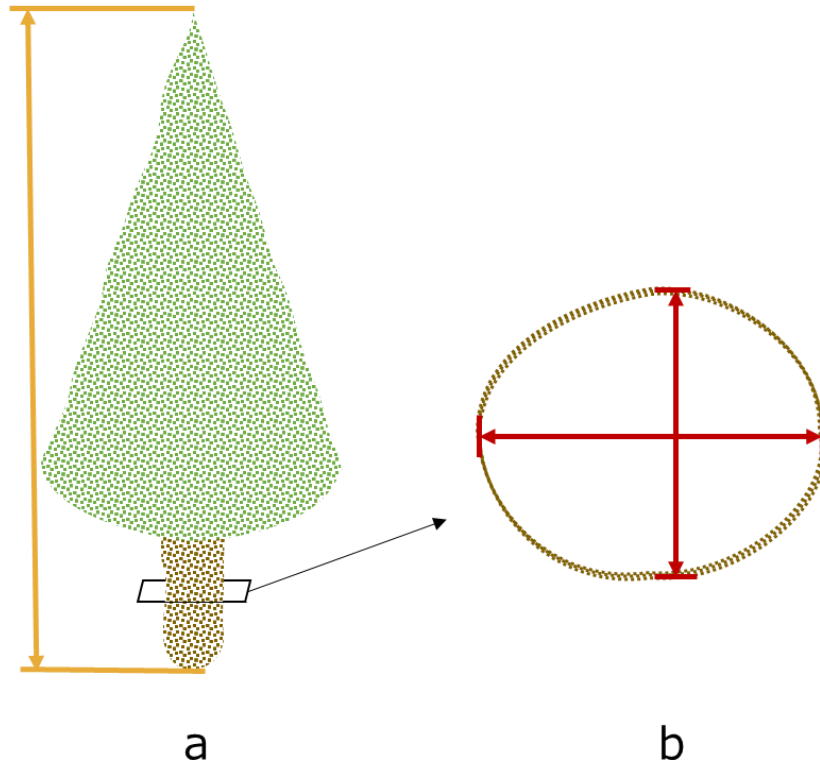


**Fig 12. Measurement methods in the generated dense clouds.  
a: Tree height measurement. b: DBH measurement**

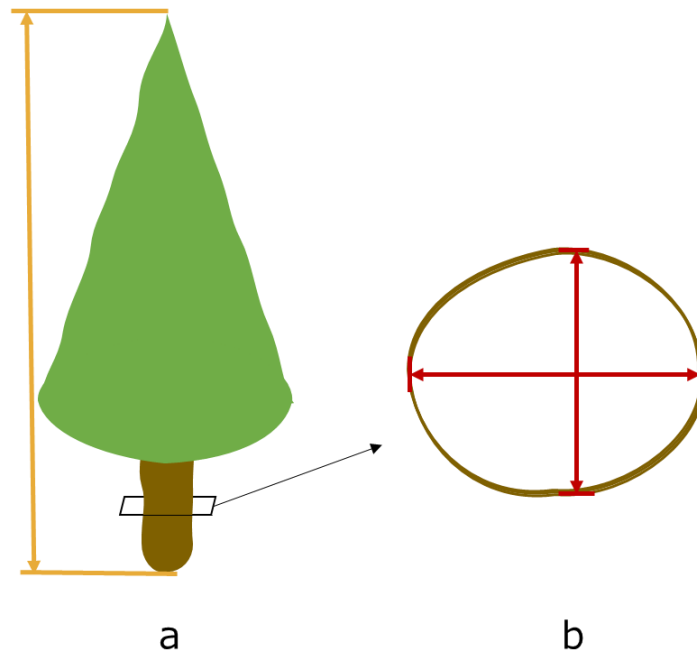


**Fig 13. Measurement methods in the generated 3D model.**  
**a: Tree height measurement. b: DBH measurement.**

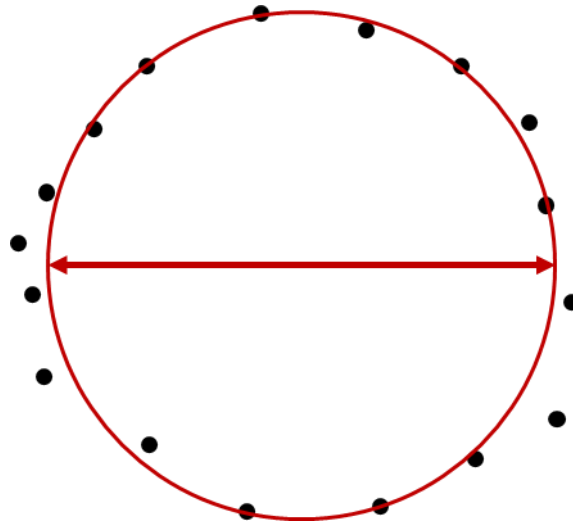


**Fig 14. Measurement method using approximate circle in the generated dense clouds and 3D models.**

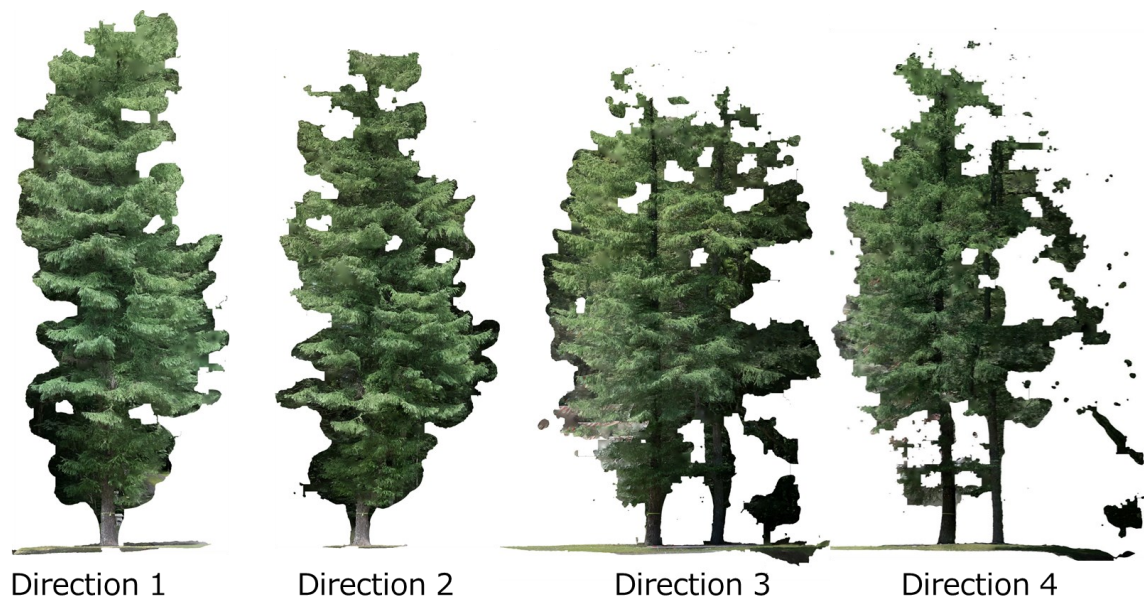


**Fig 15. Orthophotos of the Japanese larch in Mie University Forest.**

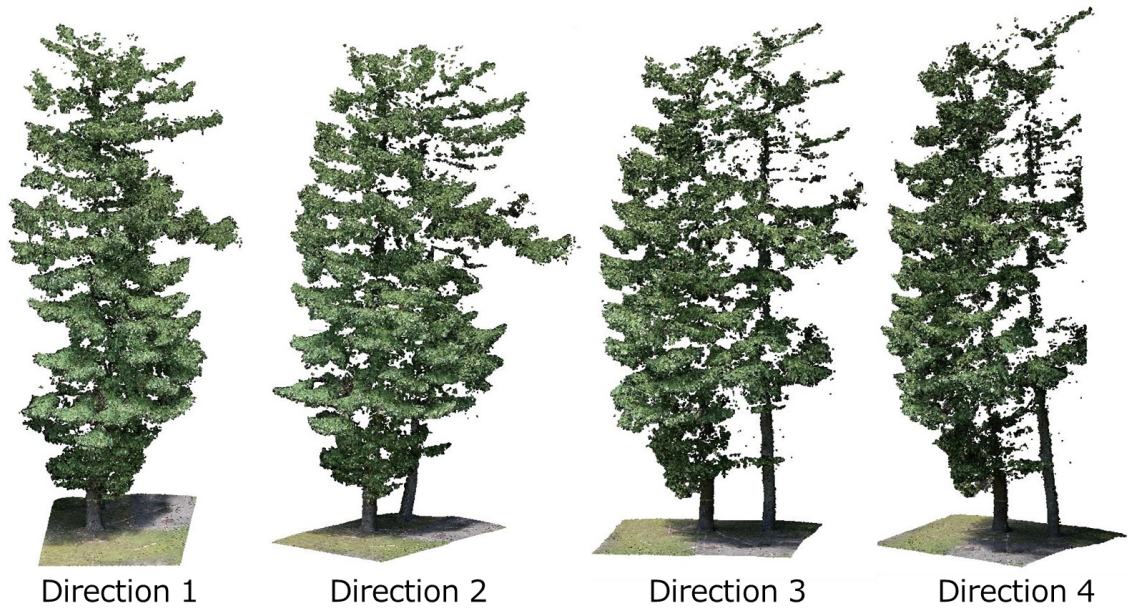


**Fig 16. Dense Cloud of the Japanese larch in Mie University Forest.**

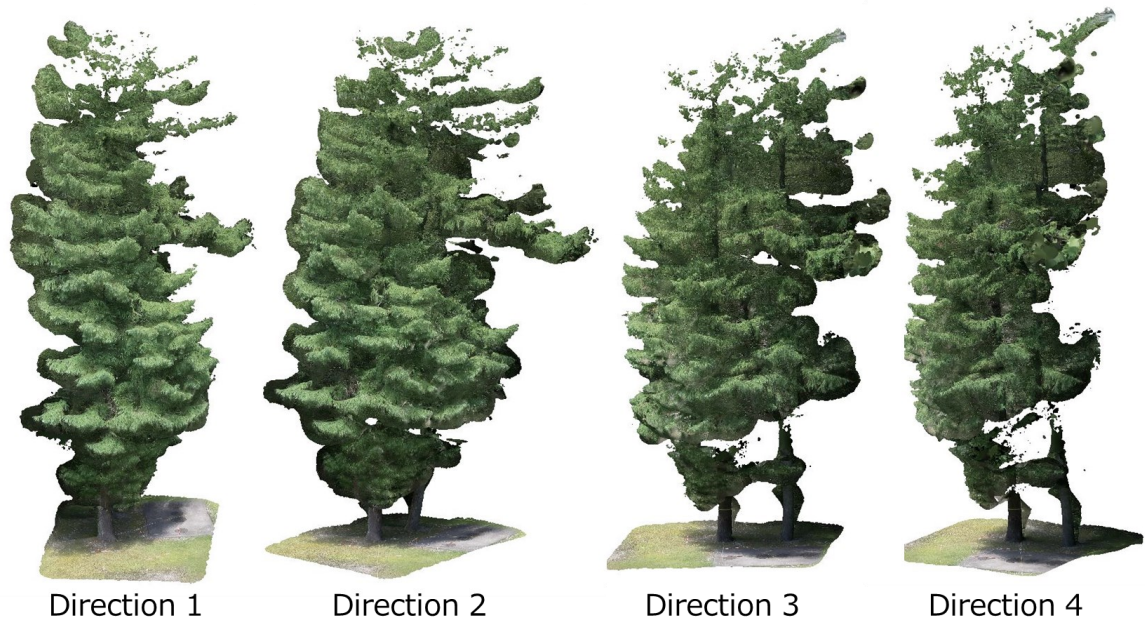


**Fig 17. 3D Model of the Japanese larch in Mie University Forest.**

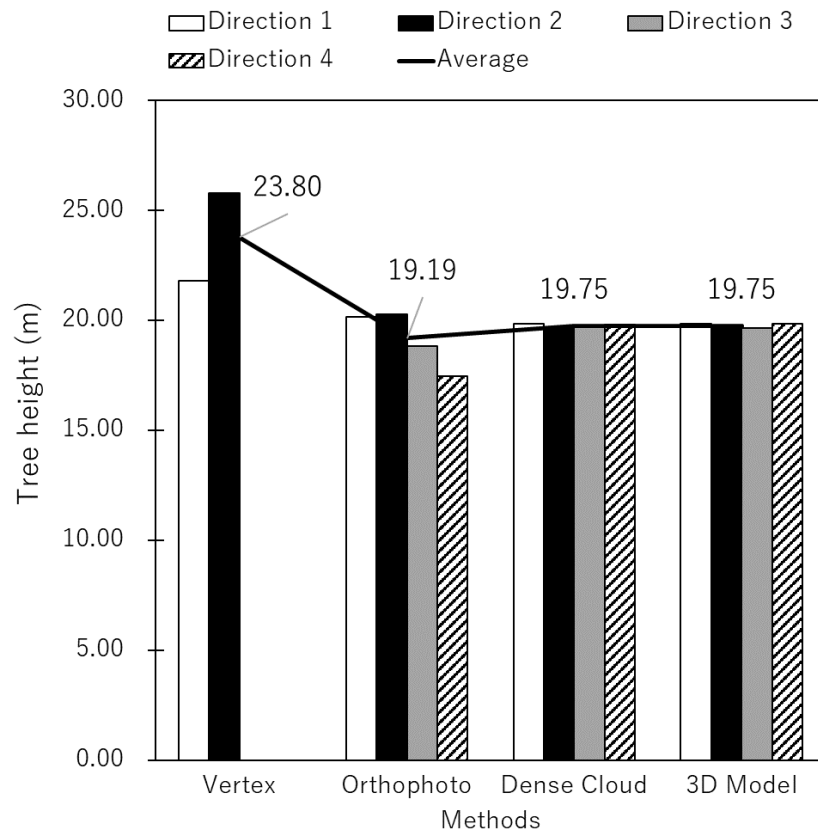


**Fig 18. Tree heights of the Japanese larch in Mie University Forest.**

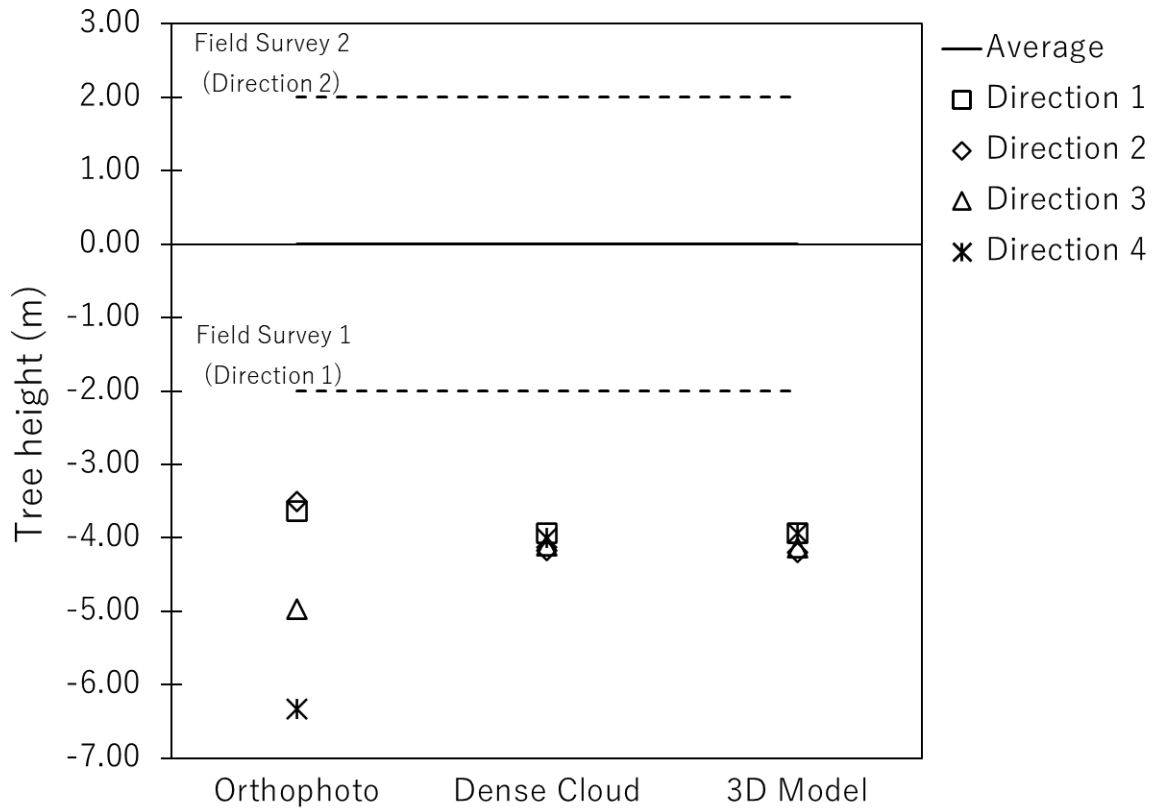


**Fig 19. Differ in the tree height measurements of the Japanese larch in Mie University Forest.**

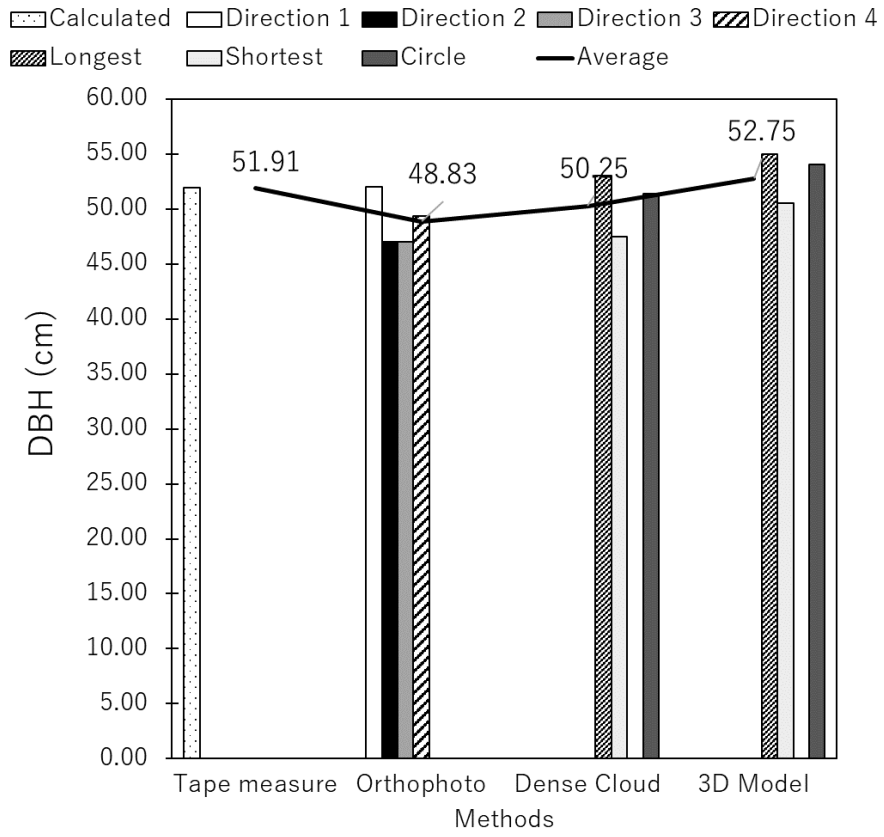


**Fig 20. DBHs of the Japanese larch in Mie University Forest.**

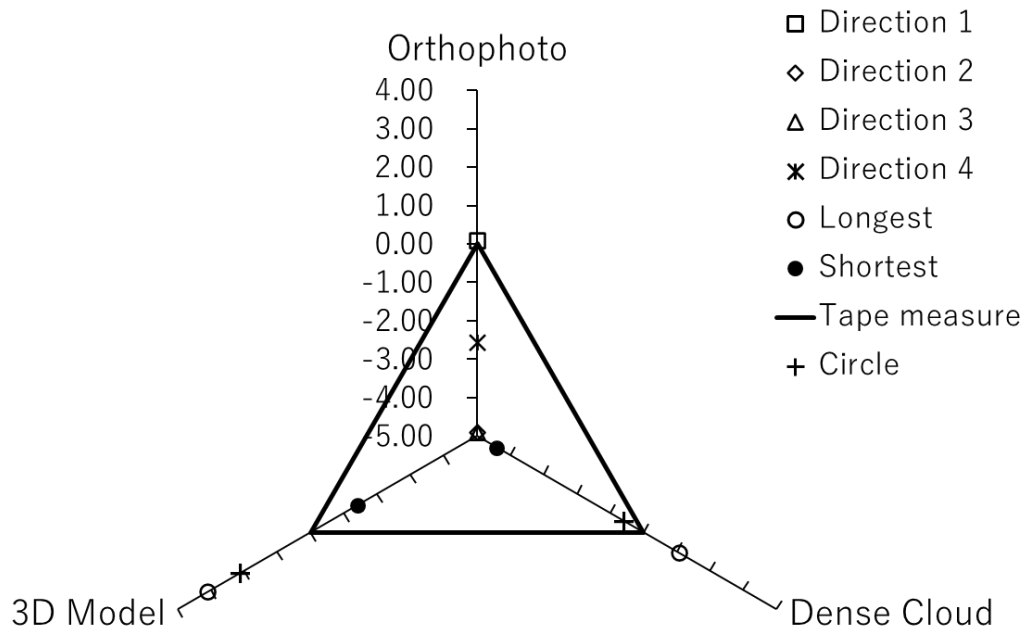


**Fig 21. Differ in the DBH measurements of the Japanese larch in Mie University Forest.**

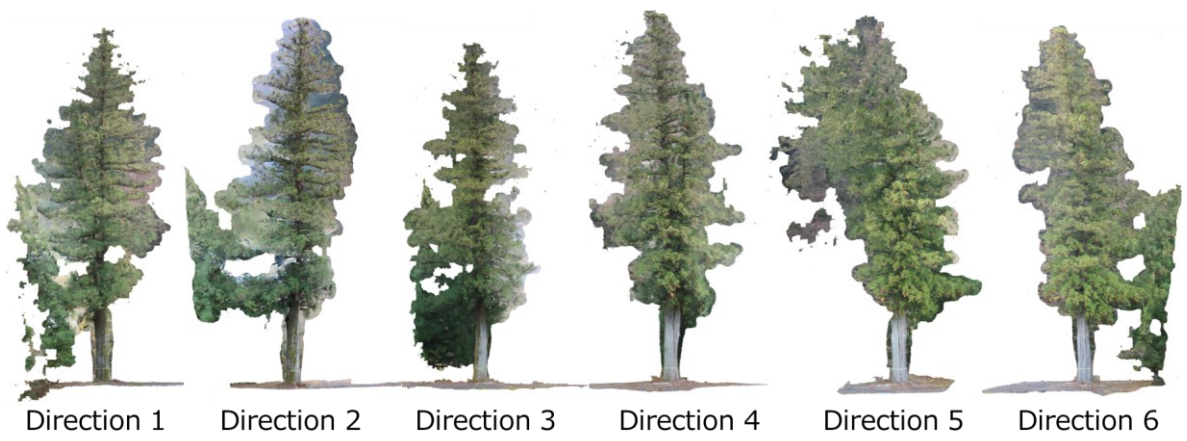


**Fig 22. Orthophotos of the Japanese cedar in Mie University Forest.**

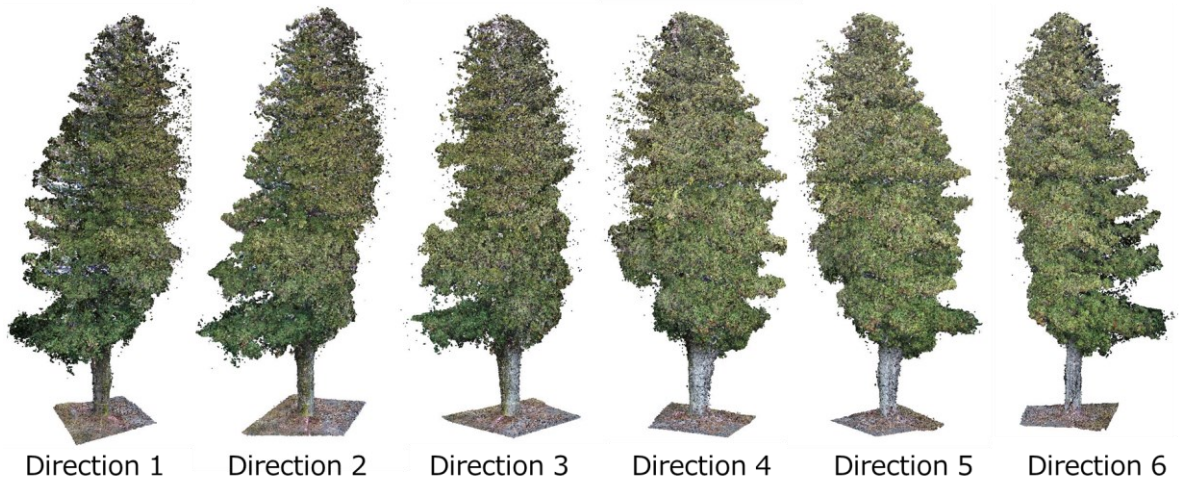


**Fig 23. Dense Cloud of the Japanese cedar in Mie University Forest.**

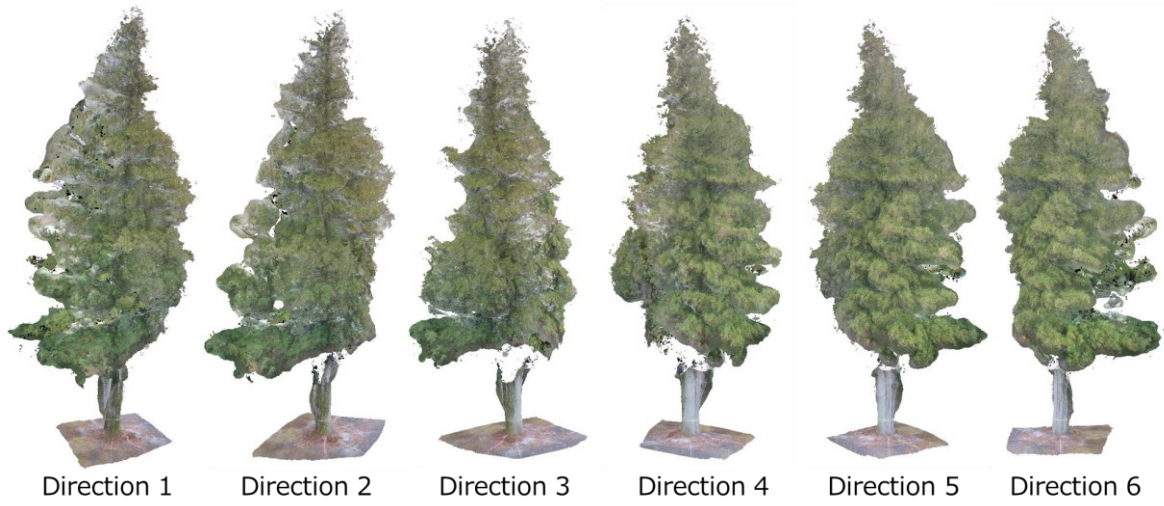


**Fig 24. 3D Model of the Japanese cedar in Mie University Forest.**

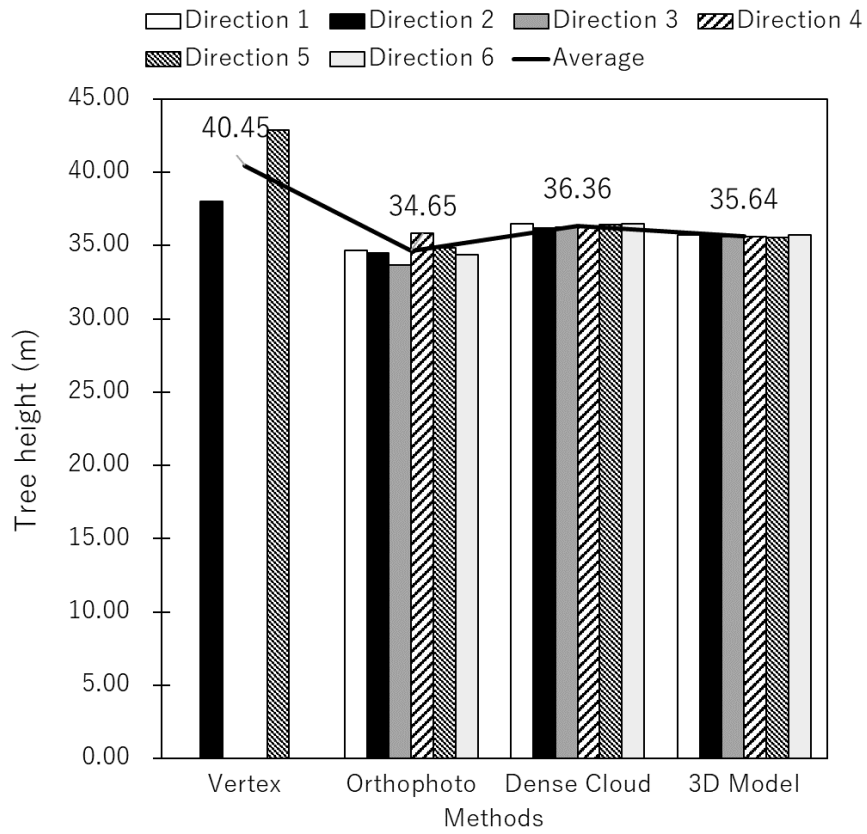


**Fig 25. Tree heights of the Japanese cedar in Mie University Forest.**

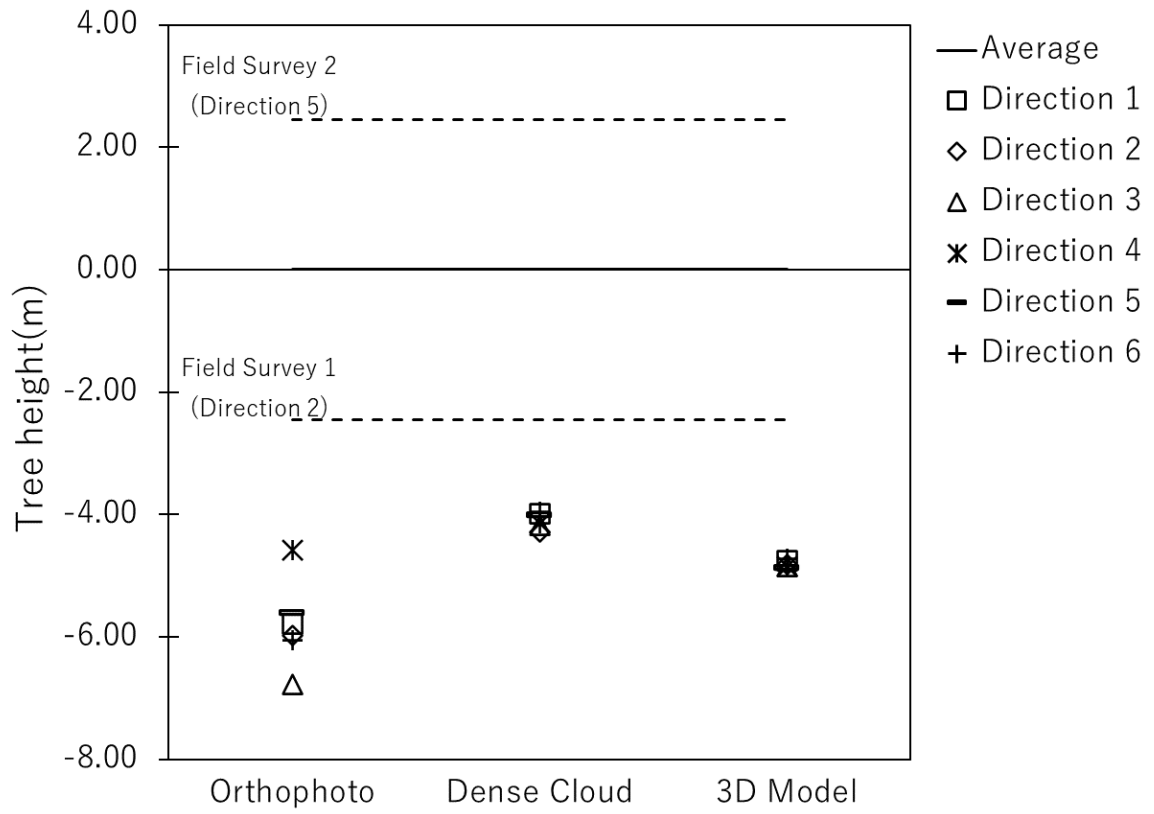


**Fig 26. Differ in the tree height measurements of the Japanese cedar in Mie University Forest.**

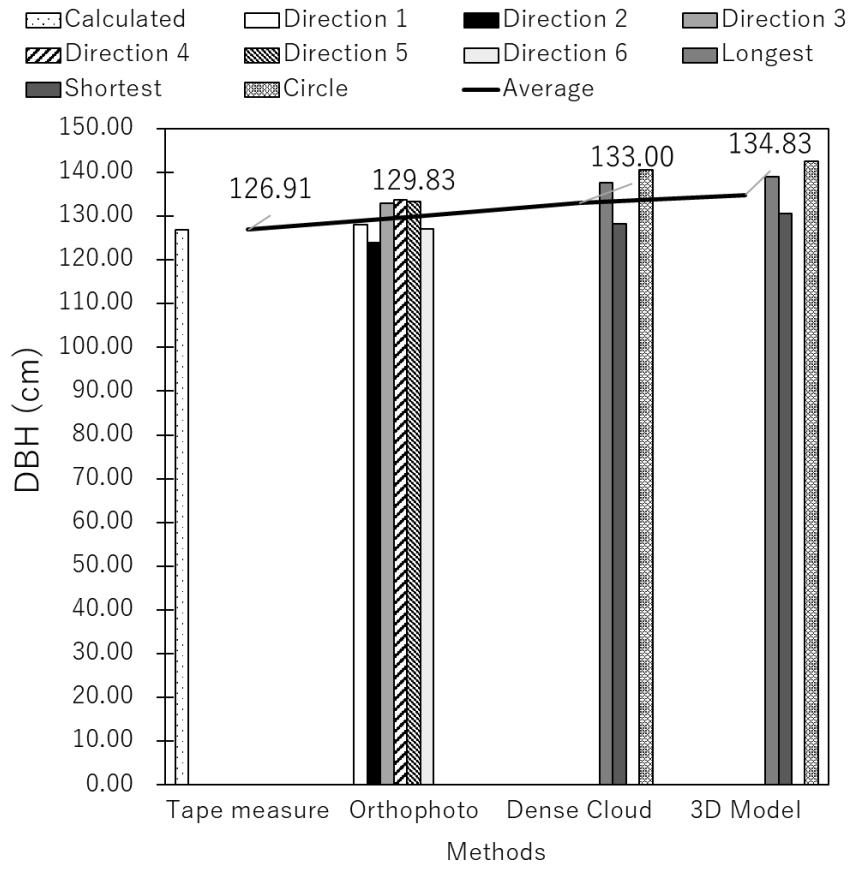


**Fig 27. DBHs of the Japanese cedar in Mie University Forest.**

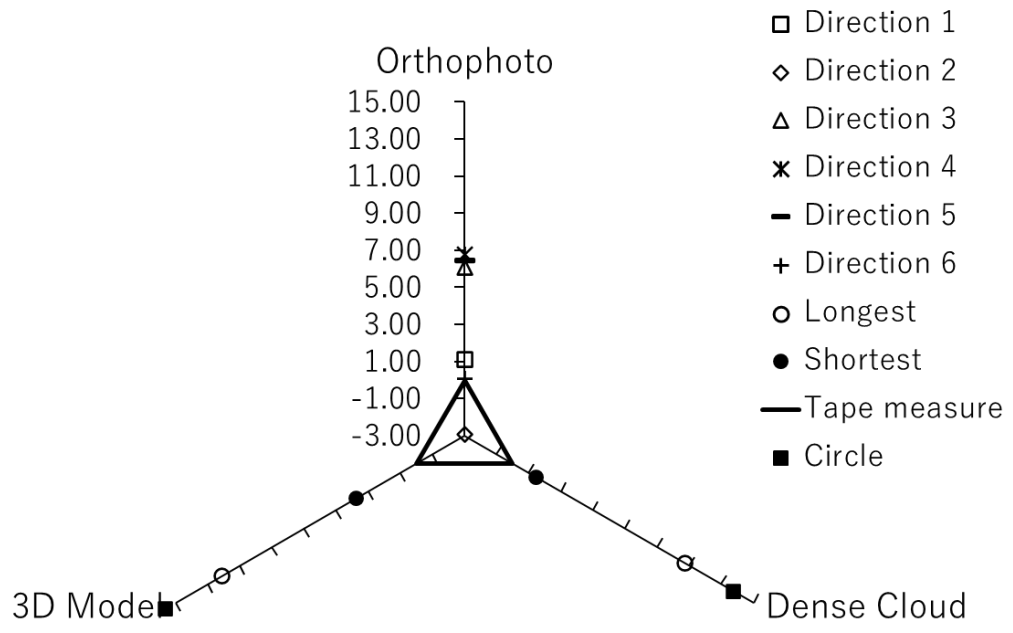


**Fig 28. Differ in the DBH measurements of the Japanese cedar in Mie University Forest.**



**Fig 29. Orthophotos of the Japanese cedar in Mt.Nonobori.**

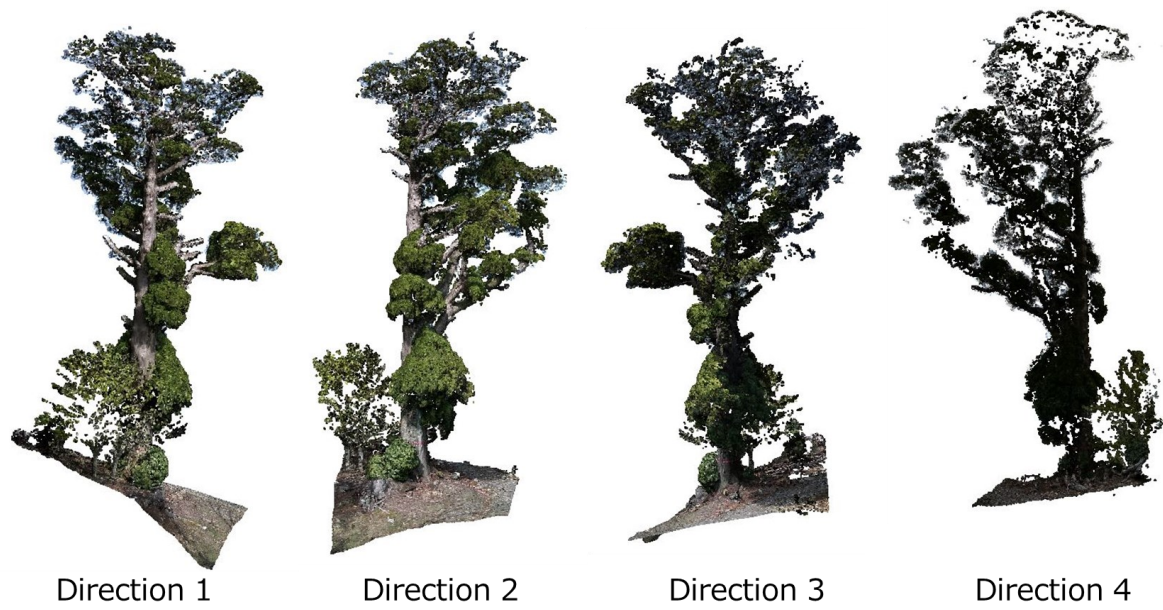


**Fig 30. Dense Cloud of the Japanese cedar in Mt.Nonobori.**

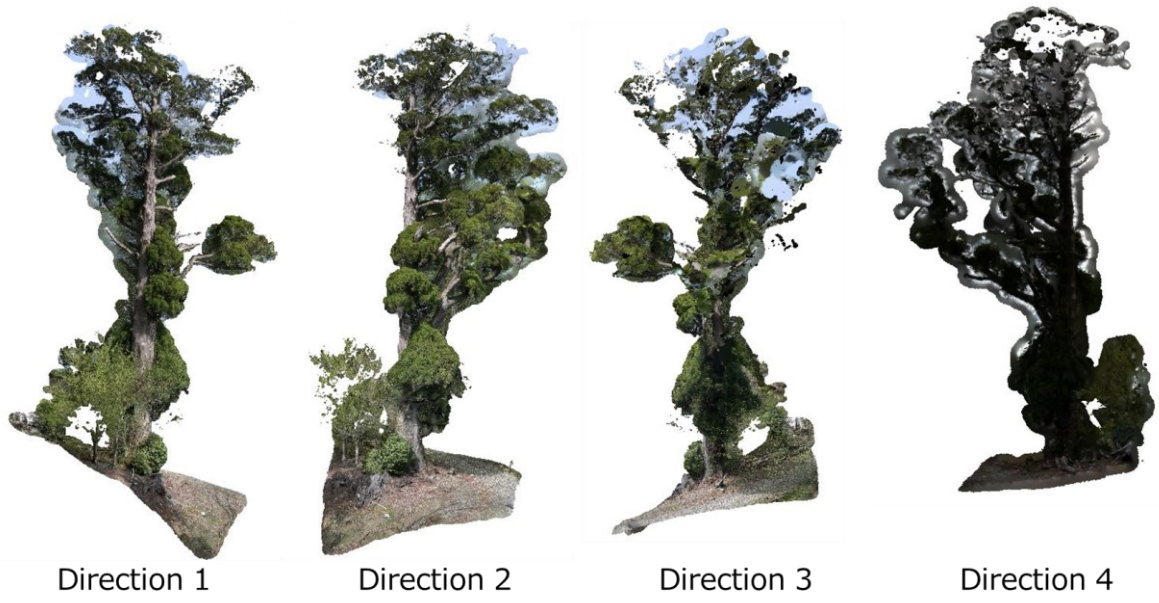


**Fig 31. 3D Model of the Japanese cedar in Mt.Nonobori.**

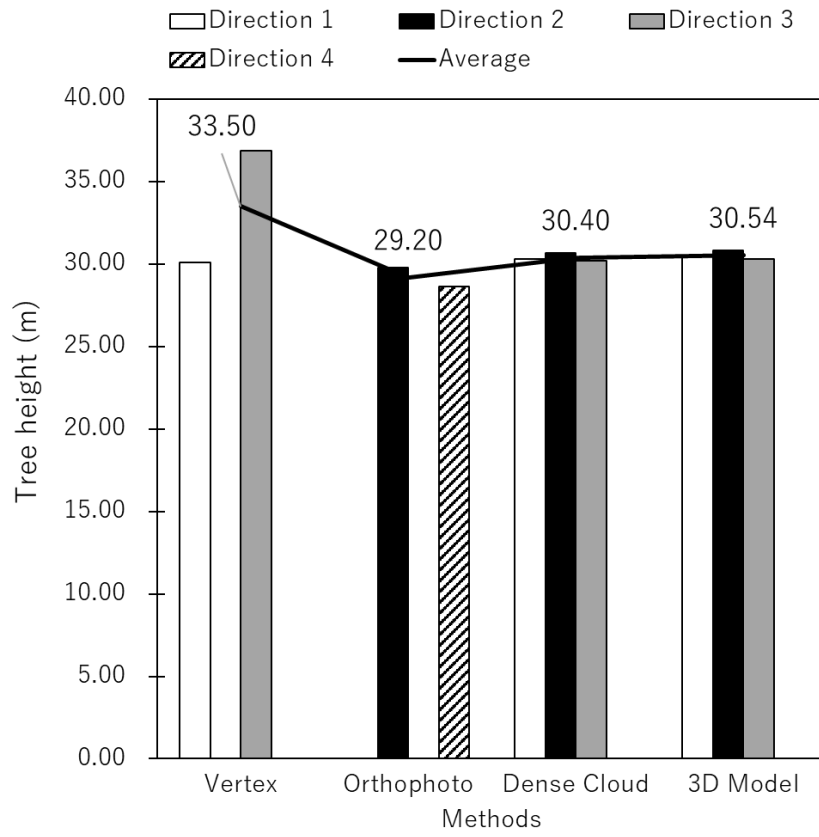


**Fig 32. Tree heights of the Japanese cedar in Mt.Nonobori.**

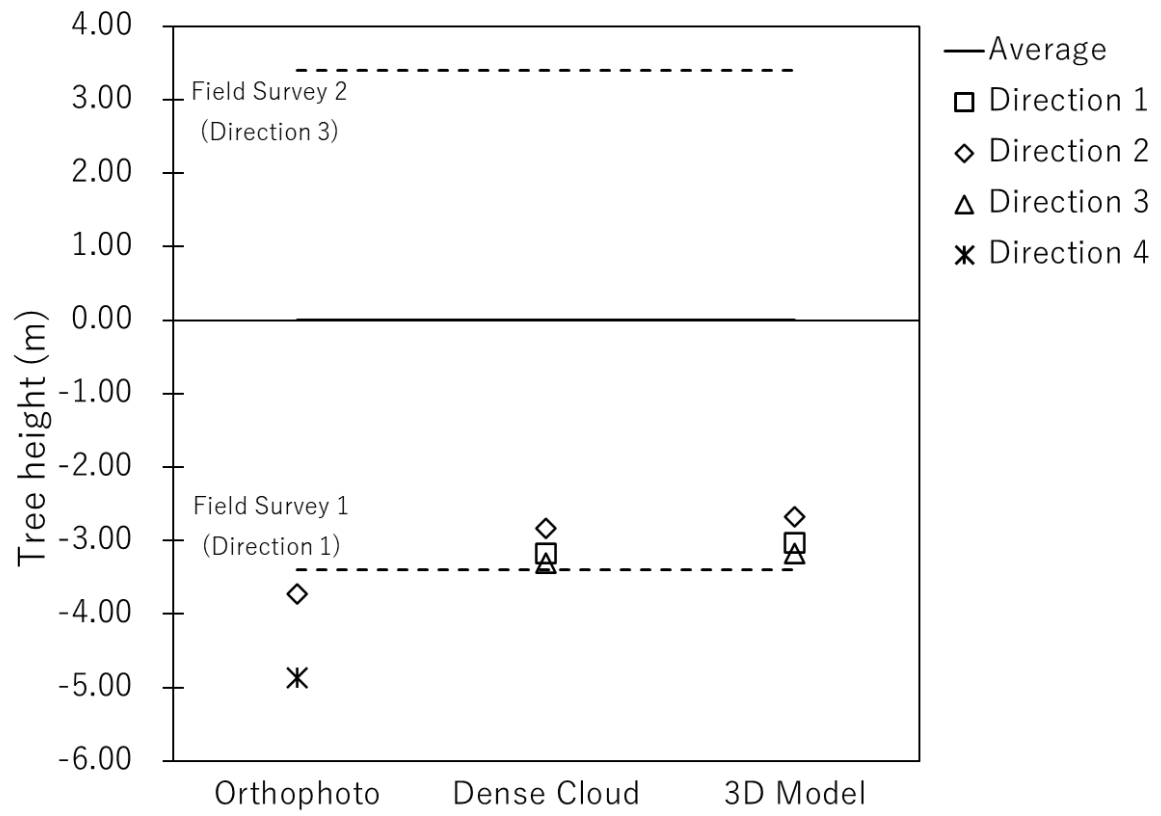


**Fig 33. Differ in the tree height measurements of the Japanese cedar in Mt.Nonobori.**

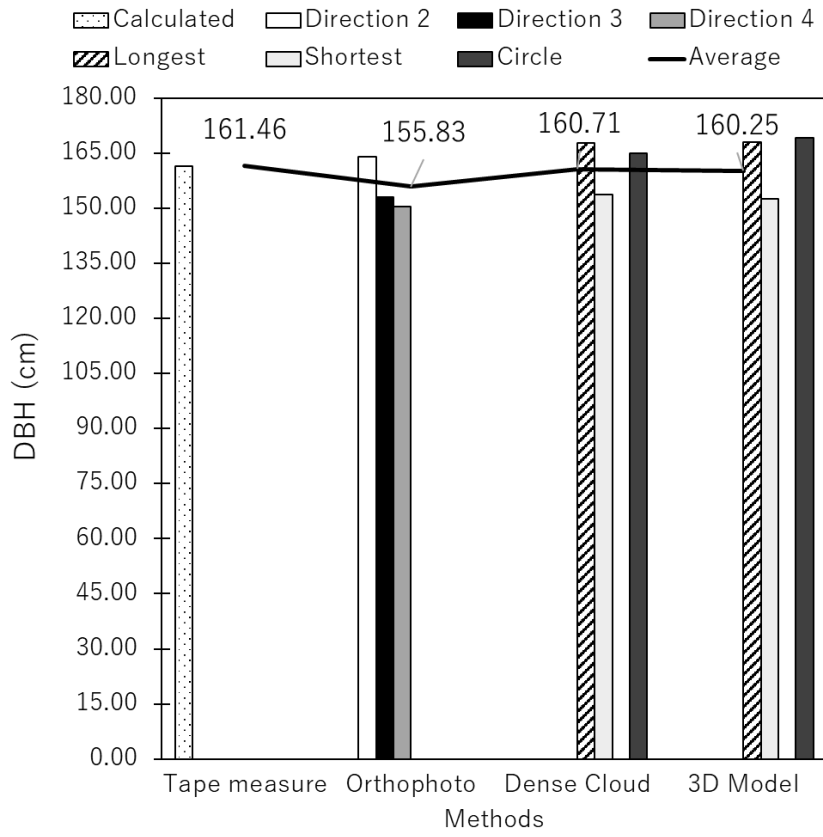


**Fig 34. DBHs of the Japanese cedar in Mt.Nonobori.**

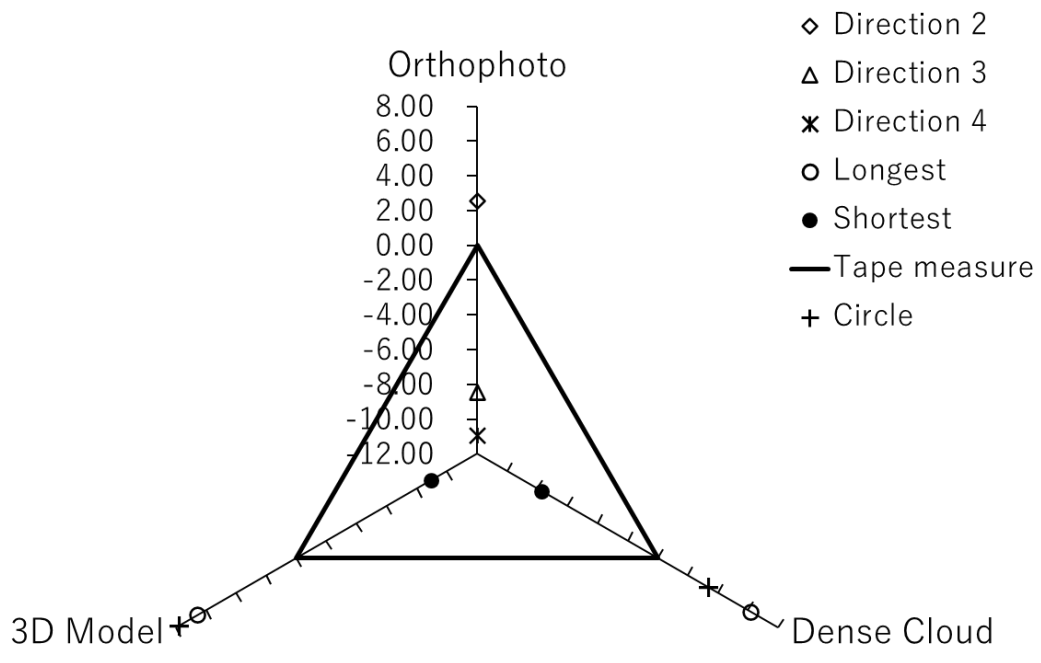


**Fig 35. Differ in the DBH measurements of the Japanese cedar in Mt.Nonobori.**